ABSTRACT

This document examines the Underlying Flow Regime (UFR) of a turbulent, axisymmetric, free-plume in a quiescent, unstratified environment. Only the far-field behaviour is considered where the buoyancy-driven plume exhibits self-similar behaviour. Another related QNET-UFR documents the unsteady turbulent behaviour near plume sources.

Turbulent, axisymmetric plumes are a feature of many important scientific and engineering applications including flows generated by smokestacks, cooling towers, fires and large geothermal events, such as volcanoes. The source of the buoyancy may be provided by temperature differences in the fluid or can be related to two fluids of different density mixing together. In some cases, the plumes originate from a source such as a pipe with some initial momentum. These flows, known as forced plumes or buoyant jets, feature jet-like behaviour near the source, a transitional region further downstream and then, even further downstream, fully-developed plume behaviour (see Figure 1).

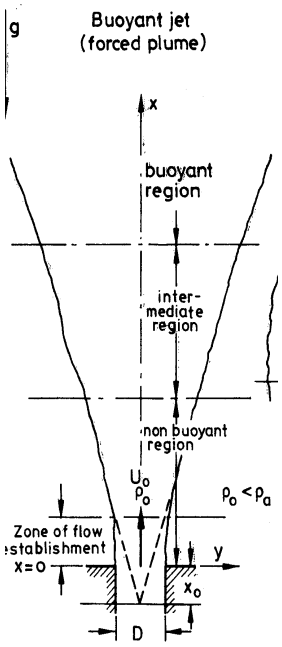

Figure 1 Flow development of a buoyant jet, from Chen & Rodi [1]

A brief review is provided in this UFR of experiments and CFD studies of fully-developed axisymmetric plumes. The recent study by Van Maele & Merci [2] is considered in some detail. Their work examined the performance of standard and realizable $k - \varepsilon$ RANS models against the experimental work of George *et al.* [3]. It showed that both standard and realizable models combined with the Generalized Gradient Diffusion Hypothesis (GGDH) for the buoyancy production term give reasonable predictions of the mean flow behaviour. The Standard Gradient Diffusion Hypothesis (SGDH) buoyancy model produces too little turbulent mixing and as a consequence underpredicts spreading rates and overpredicts mean centreline values of velocity and temperature/concentration. The conclusions from the earlier work of Chen & Rodi [1] are also discussed.

Best-practice advice is provided for CFD practitioners on key modelling issues, such as computational grid requirements and the use of simplifications, such as the Boussinesq approximation.

There is some uncertainty over the results from recent measurements reported in the literature (see Section 2.3.1). It is recommended that an in-depth review of experiments be undertaken, similar to the comprehensive study made 30 years ago by Chen & Rodi [1]. The findings of such work could affect the reported accuracy of CFD models.

1 INTRODUCTION

This document focusses on the underlying flow of the fully-developed, steady, vertical, axisymmetric (round) plume flowing in a still and unstratified environment. This includes consideration of both rising, positively-buoyant plumes and falling, dense, negatively-buoyant plumes. Only turbulent plumes are considered as this covers nearly all relevant engineering and environmental applications. For a review of laminar plumes, see [1][4][5].

This UFR is relevant to the Application Challenges AC4-03 on air flows in an open plan air-conditioned office, AC4-04 on tunnel fires, and UFR4-09 on confined buoyant plumes.

1.1 Overview of the UFR

Free vertical buoyant plumes and free-jets are related phenomena, both having a core region of higher momentum flow surrounded by shear layers bounding regions of quiescent fluid. However, whereas for jets the driving force for the fluid motion is a pressure drop through an orifice, for plumes the driving force is buoyancy due to gradients in fluid density. Plumes can develop due to density gradients caused by temperature differences, for example in fires, or can be generated by fluids of different density mixing, such as a release of hydrogen in air. There are many flows of both engineering and environmental importance that feature buoyant plumes, ranging from flows in cooling towers and heat exchangers to large geothermal events such as volcanic eruptions. For a good introduction to turbulent jets and plumes, see Chen & Rodi [1] or List [6][7]. A more general discussion of buoyant flows is given in Gebhart *et al*. [4].

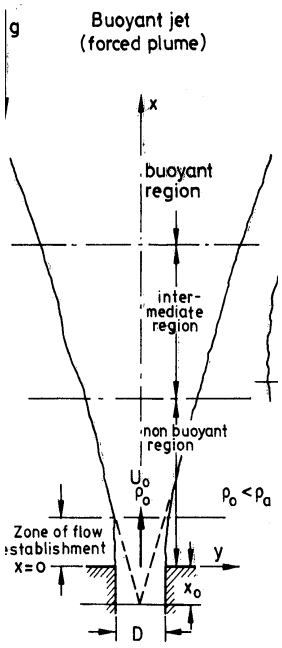

Figure 1 Flow development of a buoyant jet, from Chen & Rodi [1]

A free vertical buoyant plume can be split into a number of regions, see Figure 1. Close to the source, the flow is affected by details of the particular release conditions. This could include inertial effects if, for example, the flow involves a release of buoyant fluid through a nozzle under pressure. Other complexities near the source may be associated with combustion in fire plumes. At a sufficient distance further downstream, the effects of the source conditions are lost, buoyancy forces dominate the flow and it exhibits plume behaviour. Between the near-source and far-field regions, there is a transitional region.

Plumes arising from continuous releases of buoyant fluid with significant initial momentum are classified as *forced plumes* or *buoyant jets*. Those involving a discrete release of buoyant fluid are termed *thermals* or *puffs* (e.g. as caused by an explosion), and *starting plumes* refer to the advancing front from a continuous buoyancy source in the initial phase of the release before a steady plume becomes established.

Buoyant jets (i.e. plumes with significant initial momentum) occur in a number of important practical applications such as the flow from smokestacks and cooling-water discharges into reservoirs. It is important in these cases to be able to identify when the transition occurs from jet-like behaviour near the source to plume-like behaviour in the far field. A common dimensionless parameter used to distinguish these two flow regions is the densimetric Froude number, *Fr*, given by:

$$Fr = \frac{U}{\sqrt{\left[g\, D \left(\frac{\rho_\infty - \rho}{\rho_\infty} \right) \right]}} \tag{1}$$

where U is the mean velocity, g gravity, D a characteristic length-scale, and ρ density. Subscript ∞ refers to the far-field value[1]. The Froude number represents the ratio of inertial forces to buoyancy forces. It ranges in value from near zero for pure plumes, towards infinity for jets with negligible buoyancy. Chen & Rodi [1] analysed a number of jet and plume experiments and, using dimensional analysis, produced the graph reproduced in Figure 2, which shows the transition from jet- to plume-like behaviour with increasing Fr[2].

Figure 2 shows how the difference in mean density between the axis of the plume and the far field value decays with distance from the inlet. In the jet-like region near the source, the density difference decays at a rate $(x - x_0)^{-1}$ whereas in the fully-developed plume region it decays faster at $(x - x_0)^{-5/3}$. Here, x is the axial coordinate and x_0 is the "virtual" source location, see Figure 1. Empirical correlations for the decay rate of mean velocity and scalars in buoyant jets are given in Gebhart *et al*. [4]. Both jets and plumes spread linearly in a uniform environment, although at different rates. Empirical correlations for the spreading rate in plumes are given later.

Another common measure used to assess when buoyant jets reach a fully-developed state is the Morton length scale, l_M:

$$l_M = \frac{M_0^{3/4}}{F_0^{1/2}} \tag{2}$$

1 In some cases, the densimetric Froude number is defined with the density difference made dimensionless using the plume source density, ρ, instead of the ambient density ρ_∞, e.g. Chen & Rodi [1] and Hossain & Rodi [8].

2 The local Froude number in this case is evaluated on the plume centreline. Note, the *Fr* defined by Chen & Rodi [1] is the square of the definition of *Fr* given above.

where M_0 and F_0 are the specific momentum and buoyancy added at the source of the plume:

$$M_0 = 2\pi \int_0^{r_0} U^2 r\, dr \qquad\qquad F_0 = 2\pi \int_0^{r_0} Ug \frac{\Delta\rho}{\rho_\infty} r\, dr \tag{3}$$

For plumes with uniform properties at the source, this is equivalent to:

$$l_M = \frac{Fr_0 D}{(\pi/4)^{1/4}} \tag{4}$$

where Fr_0 is the the source densimetric Froude number at the source and D the inlet source diameter.

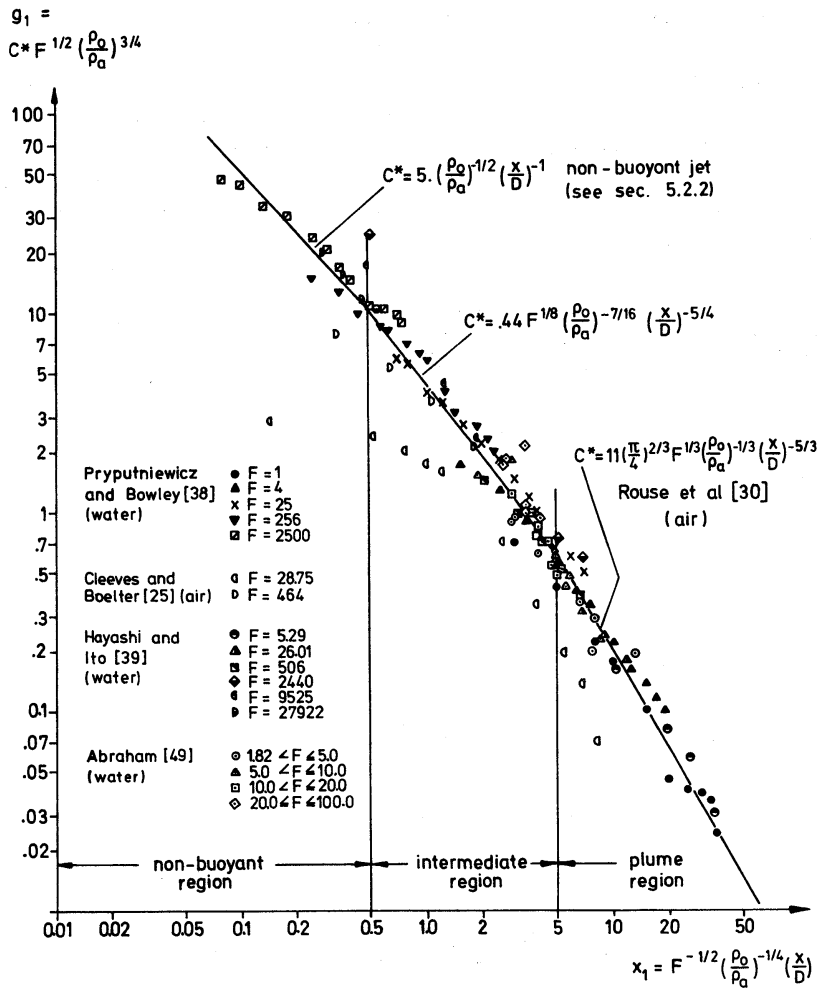

Figure 2 Decay of centreline density in round plumes from Chen & Rodi [1]

Papanicolau & List [9] suggest that jet-like conditions occur in turbulent buoyant jets for $(x-x_0)/l_M < 1$ and fully-developed plume-like conditions for $(x-x_0)/l_M > 5$. However, there is some debate in the literature over the distance required to reach fully-developed plume conditions,

see for example Dai *et al*. [10] and Shabbir & George [11]. Mean parameters (velocity, temperature etc.) require a shorter distance to reach a fully-developed state than statistical quantities such as Reynolds stresses.

An important feature of the mean flow in the fully-developed region of turbulent buoyant plumes is "self-similarity" or "self-preserving" behaviour. In positively-buoyant plumes, as the less dense fluid rises and spreads, the mean velocity peak on the plume centreline decays and the plume becomes wider. However, the shape of the mean velocity profile remains the same. If the dimensionless radial profiles of the mean velocity are plotted at different vertical positions in the plume on the same graph axes, the curves all fall on top of one another. Self-similarity is also exhibited in the dimensionless temperature and species concentration profiles and in the dimensionless RMS turbulent fluctuations of velocity, temperature and concentration ($\sqrt{\overline{u^2}}/U_0$, $\sqrt{\overline{v^2}}/U_0$, $\sqrt{\overline{\theta^2}}/\Theta_0$ or $\sqrt{\overline{c^2}}/C_0$). Sample data from the experiments of Papanicolaou & List [9] and Dai *et al*. [10] shown in Figures 3 and 4 demonstrate this behaviour.

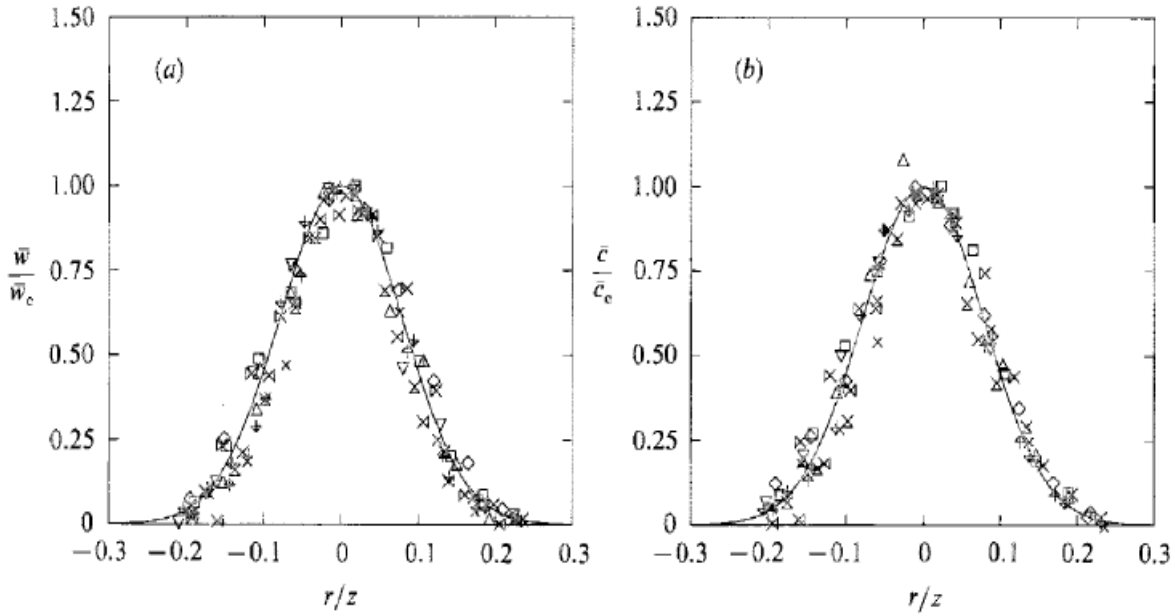

Figure 3 Dimensionless mean velocity and mean concentrations profiles in a turbulent axisymmetric plume, from Papanicolaou & List [9].

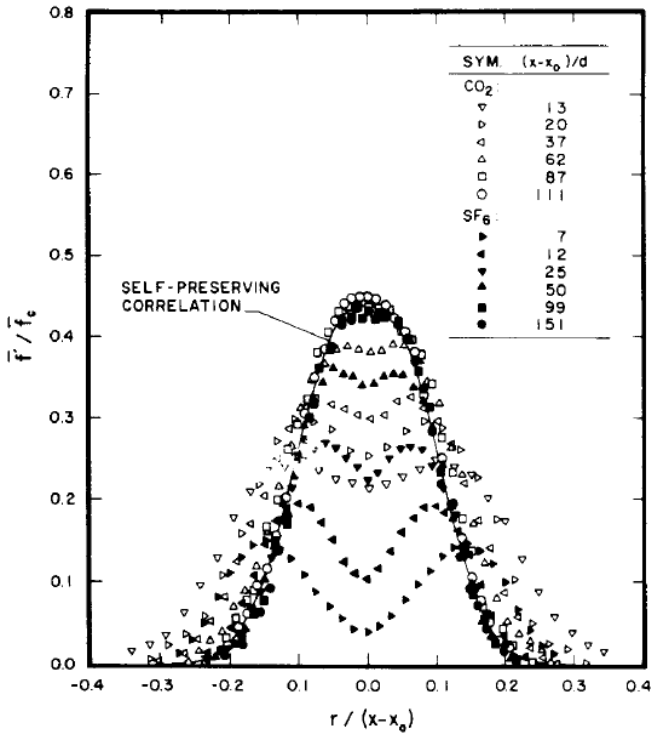

Figure 4 Dimensionless mixture fraction fluctuation profiles in a turbulent axisymmetric plume, from Dai *et al*. [10]

1.1.1 Plume Analysis Based on Integral Equations

One means of analysing the flow behaviour of self-similar buoyant plumes is to use integral methods. This involves assuming profiles for the velocity, temperature and concentration based on experimental observations. The mean flow equations are then integrated over the whole plume cross-section to produce ordinary differential equations. The entrainment rate is also assumed, usually as a function of the local centreline velocity.

Theoretical analysis of self-similar plumes using integral methods began more than 50 years ago with the works of Yih [12], Rouse *et al*. [13], Batchelor [14] and Morton *et al*. [15] for plumes with small density differences in unstratified and stratified environments. More recently, these theories have been extended to consider plumes with significant density differences [16][17], with unsteady source strengths [18][19][20] and fire plumes [21][22][23][24].

The simplest analysis proceeds by assuming that the velocity and buoyancy force are constant across the plume and zero outside it (i.e. a 'top hat' profile). Transport equations for the conservation of volume, momentum and density deficit are integrated analytically with respect to the vertical distance, x, to arrive at expressions for the plume radius, b, the vertical velocity, U, and the density, ρ, inside the plume:

$$b = \frac{6}{5}\alpha x \qquad U = \frac{5}{6\alpha}\left(\frac{9}{10}\alpha Q\right)^{1/3} x^{-1/3} \qquad g\frac{(\rho_1 - \rho)}{\rho_1} = \frac{5Q}{6\alpha}\left(\frac{9}{10}\alpha Q\right)^{-1/3} x^{-5/3} \tag{5}$$

where ρ_1 is a reference density, α is an empirical entrainment coefficient and Q is the buoyancy flux, given by:

$$Q = b^2 U g\left(\frac{\rho_1 - \rho}{\rho_1}\right) \tag{6}$$

The empirical entrainment coefficient, α, relates the entrainment velocity, U_e, to the plume velocity ($U_e = \alpha U$). This analysis was first published by Schmidt [25] and is described in Morton *et al*. [15].

Morton *et al*. [15] extended the above approach, assuming Gaussian radial profiles for the velocity and buoyancy force instead of top-hat profiles. They found that the spreading rate of the plume ($\mathrm{d}b/\mathrm{d}x$) was equal to $6\alpha/5$ and was independent of the strength of the buoyancy source. In their analysis they defined the plume radius, b, as the point where the velocity fell to e^{-1} of its centreline value ($0.37U_c$). Experiments undertaken by Morton *et al*. [15] of positively buoyant plumes in stratified saline solutions found the entrainment coefficient to be around $\alpha = 0.093$. More recent studies have suggested a value of $\alpha \approx 0.082$ for plumes in unstratified environments (for comparison, the entrainment constant for pure jets is $\alpha \approx 0.057$) [4][26].

Recently, Diez & Dahm [27] developed an alternative integral approach that does not rely upon the entrainment coefficient, α. Instead, it uses the integral equation for the momentum flux to develop an equation for the local centreline velocity. Diez & Dahm's model relies upon a parameter, c_δ, which experiments show to be constant in the far-field of both jets and plumes.

Further details of integral methods applied to plumes and jets, including discussion of empirical models for α as a function of the Froude number, can be found in Chen & Rodi [1] and Gebhart *et al*. [4].

Whilst integral methods can provide accurate results for relatively simple plumes it is difficult to extend the approach to model more complex turbulent flows, where for example the plume may hit a wall or encounter regions of flow recirculation. To study these more complex flows, a more general-purpose CFD approach must be used.

1.2 Review of UFR Studies and Choice of Test Case

CFD simulations of fully-developed, self-similar turbulent buoyant plumes have, to date, mainly solved the Reynolds-Averaged Navier Stokes (RANS) equations. Whilst Large Eddy Simulation (LES) can in theory be used to study such flows, it involves significantly greater computing resources. To the authors knowledge, the only study of the far-field, self-similar behaviour of plumes using LES is that undertaken by Zhou *et al*. [28][29]. They simulated the thermal plumes of George *et al*. [3] and Shabbir & George [11] in [28] and those of Cetegen [30] in [29]. Whilst axisymmetric RANS simulations of these flows would involve meshes with around 4,000 cells, the large-eddy simulations of Zhou *et al*. [28][29] used more than 4 million cells.

Before describing the experimental and CFD studies on which this UFR documentation will be based, a brief review is provided below of other studies of the axisymmetric buoyant plume which, for various reasons, have not been adopted here.

1.2.1 Review of the nearly-relevant work

Experiments

There have been numerous experimental studies of the turbulent buoyant plume. A major review was undertaken by Chen & Rodi in 1980 [1]. They provided recommended values for the spreading rates of the plume based on the momentum and temperature or concentration of $dr_{U1/2}/dx = 0.112$ and $dr_{f1/2}/dx = 0.104$. The momentum value $\left(dr_{U1/2}/dx\right)$ was based on the experiments of George *et al*. [3] which were considered to be the most consistent of the reviewed data.

Following Chen & Rodi's review, in the late 1980's and early 90's, Shabbir, George and Taulbee at the University of Buffalo published a number of papers on buoyant plume experiments [31][32][33] [34]. In [33] they compared the magnitude of various terms in the $k - \varepsilon$ model equations to values obtained directly from experiments. A particularly significant finding was that the streamwise heat flux, $\overline{uT}$, was underpredicted by a factor of four using the standard $k - \varepsilon$ model with the Simple Gradient Diffusion Hypothesis (SGDH) (described later). Apart from this shortcoming, however, the $k - \varepsilon$ model was found to perform reasonably well.

More recently, Dai *et al*. [10] performed experiments using negatively-buoyant plumes of CO_2 and SF_6 in air. A summary table, comparing their results for the axisymmetric buoyant plume against those of Papantoniou & List [35], Papanicolaou & List [9][36], Shabbir & George [34] and George *et al*. [3] is reproduced in Table 1a.

Table 1a Summary of self-preserving buoyant plume properties, from Dai *et al*. [10]

Source	Medium	$(x-x_0)/d$	$(x-x_0)/\ell_M$	k_f^2	$\ell_f/(x-x_0)$	F(0)	$(\bar{f}'^2/\bar{f})_c$
Present study	gaseous	87-151	12-43	125	0.09	12.6	0.45
Papantoniou and List (1989)	liquid	105	24,33	---	0.08-0.09	---	0.64
Papanicolaou and List (1988)	liquid	22-62	9-62	80	0.11	14.3	0.40
Papanicolaou and List (1987)	liquid	12-20	> 5	80	0.11	11.1	0.40
Shabbir and George (1992)	gaseous	10-25	6-15	68	0.12	9.4	0.40
George et al. (1977)	gaseous	8-16	6-12	65	0.12	9.1	0.40

[a]Round turbulent plumes in still, unstratified environments. Range of streamwise distances are for conditions where quoted self-preserving properties were found from measurements over the cross section of the plumes. Entries are ordered in terms of decreasing k_f.

Table 1b Densimetric Froude numbers for the experiments given in Table 1a, calculated using Equation (1).

Source	Fr_0
Dai et al. [10]	3.75, 7.80
Papantoniou and List (1989)	1.89, 2.24
Papanicolaou and List (1988)	0.87 to 3.88
Papanicolaou and List (1987)	0.41 to 7.79
Shabbir and George (1992)	1.60, 1.80
George et al. (1977)	1.23

The third and fourth columns of Table 1a define the extent of the fully-developed flow regions in the axial direction made dimensionless using the source diameter, d, and the Morton length scale, $l_{M.}$. Dai *et al*. [10][37][38][39], suggested that the large range in values of $(x - x_0)/l_M$ shown in Table 1a is due to the fact that many researchers had incorrectly made measurements of transitional plumes exhibiting quasi-jet-like behaviour, rather than fully-developed, self-similar plumes. They attributed this partly to the difficulty in measuring concentrations accurately at significant distances from the source due to the relatively fast $(x - x_0)^{-5/3}$ decay rate of scalars in plumes. They also noted that flow velocities in plumes are relatively low compared to jets, and so greater care had to be taken in the far field to prevent small external disturbances affecting measurements.

This matter was disputed by Shabbir & George [11] and George [40] who noted that plume measurements are strongly influenced by ambient thermal stratification. Since stratification is more difficult to control the further ones goes from the source, this could potentially affect measurements taken at larger axial distances, such as those taken by Dai *et al*. [10][37][38][39] at distances of z/D up to 151. In a neutral environment, conservation of energy implies conservation of buoyancy [1]. One means to check whether ambient thermal stratification has adversely affected measurements is therefore to ensure that buoyancy is conserved. Shabbir & George [11] carefully determined the rate of buoyancy added at the source and found that in their measurements, buoyancy was conserved to within 10%.

The other columns in Table 1a provide details of the shape of the self-similar profiles of the scalar within the fully-developed region. The radial mean scalar profiles were approximated using a Gaussian profile:

$$F\left(\frac{r}{x-x_0}\right)=F(0)\exp\left[-k_f{}^2\left(\frac{r}{x-x_0}\right)^2\right] \tag{7}$$

To obtain self-similar profiles, the mean properties were then scaled using the following formula, from List [6]:

$$\overline{f}=\left(\frac{\pi Fr_0}{4}\right)^{2/3}\left(\frac{\rho}{\rho_0}\right)\left(\frac{x-x_0}{D}\right)^{-5/3}F\left(\frac{r}{x-x_0}\right) \tag{8}$$

The final two columns in Table 1a provide centreline values of the dimensionless mean scalar, $F(0)$, and RMS scalar fluctuations, $(\overline{f'}/\overline{f})_c$, for the various experiments. The sixth column provides

details of the spreading rate of the plume, denoted $l_f/(x-x_0)$, where l_f is the plume radius as defined by the point where $\overline{f}$ falls to e^{-1} of its centreline value.

The experiments undertaken by Dai *et al*. [10][37][38][39] indicated that self-similar round turbulent plumes were up to 40% narrower and had mean centreline scalar values and streamwise velocities that were up to 30% larger than were previously thought. This finding was confirmed by a later study by the same group using the same experimental arrangements [41]. The paper by Brescianini & Delichatsios [42] provides cross-plots of both Dai *et al*. [10] and George *et al*. [3] velocity profiles. These show that on a graph of velocity, U, versus radial location $r/(x - x_0)$, the experimental profile from George *et al*. [3] is significantly flatter and wider than the more recent data of Dai *et al*. [10]. However, when plotted in dimensionless form (U/U_c versus $r/r_{1/2}$) the data are remarkably similar.

In 1994, Shabbir & George [11] repeated the earlier experiments of George *et al*. [3] with the joint aim of reproducing the earlier experiments under stricter laboratory conditions and investigating the budgets of the mean energy and momentum equations. The peak mean values and plume half-widths were found to be in good agreement with their earlier work (see also Heskestad [43] for comparisons). Shabbir & Taulbee [44] recently provided further analysis of the budgets for the turbulent heat flux and Reynolds stress transport equations to help with the development of new second-moment closure models. They found that the "local equilibrium assumption" (where production and dissipation are in balance) provided a reasonable approximation for the turbulent heat flux transport equation but that convection and diffusion terms were significant in the Reynolds stress budgets. This finding has implications for the development of algebraic stress models (see later). *A priori* assessment of simple pressure-correlation models for the turbulent heat flux and Reynolds stress equations were also presented in [44]. They found that the measured axial heat flux, $\overline{uT}$, was generally several times larger than that modelled by a simple Boussinesq gradient diffusion form and proposed an algebraic stress model to improve its prediction.

A recent experimental study by Yao & Marshall [45] used Planar Laser Induced Fluorescence (PLIF) to investigate turbulent buoyant salt-water plumes. Results were given for the fully-developed region extending approximately from $6 < (x - x_0)/D < 30$, where the mean plume radius was found to increase linearly and the dimensionless density difference decay according to the -5/3 law. Velocity measurements were not made. Dimensionless RMS concentration fluctuations varied between 0.35 and 0.45, in fair agreement with the earlier experiments reported in Table 1a. The purpose of Yao & Marshall's measurements was to simulate fire plumes. However, as they noted, care should be taken in interpreting data from salt-water experiments since the Schmidt number in liquid plumes is nearly three orders of magnitude larger than the corresponding value in gaseous plumes. The effect of this higher Schmidt number is to inhibit scalar mixing at small scales and near walls, where molecular diffusion is significant.

The review paper by Heskestad [43], discussed briefly the variability in reported measured peak values and spreading rates in axisymmetric plume experiments, shown in Table 2. Heskestad's earlier fire plume measurements [22], were in reasonably good agreement with the measurements of George *et al*. [3]. For the spreading rate of the plume, Heskestad [43] commented that the George *et al*. [3] and Shabbir & George [11] experiments were considered the most reliable. Chen & Rodi [1] also considered the work of George *et al*. [3] to be the most consistent of their reviewed data.

Table 2 Summary of experimental plume characteristics from Heskestad [43]

Study	*Centreline velocity, U_0*	*Half-width based on velocity, b_U*	*Centreline temperature difference, ΔT_0*	*Half-width based on temperature, $b_{\Delta T}$*
Heskestad [22]	3.4	-	9.1	0.12
George *et al*. [3]	3.4	1.08	9.1	0.104
Shabbir & George [11]	3.4	1.07	9.4	0.10
Papanicolaou & List [9]	3.9	-	14.3	0.09
Dai *et al*. [10]	-	-	12.6	0.08

CFD Studies

One of the most comprehensive early CFD studies of buoyant plumes was undertaken by Hossain & Rodi [8]. They examined the performance of an algebraic stress and heat flux model in axisymmetric and plane plumes, buoyant jets and pure jets. Their model was based on the differential stress model of Gibson & Launder [46] which is described in some detail in their paper. They showed how the differential model was simplified to algebraic expressions by neglecting the convective and diffusive fluxes, effectively assuming that the flow only evolves slowly (i.e. local equilibrium). The validity of this assumption in buoyant plumes was examined subsequently by Shabbir & Taulbee [33]. The proposed algebraic model shared some features with the standard $k - \varepsilon$ model but used modified expressions for the stresses and heat fluxes and a more sophisticated diffusion term. An important feature of the model was that the coefficients appearing in the eddy viscosity and diffusivity were functions of buoyancy parameters (not the case with the standard $k - \varepsilon$ model). The model also incorporated an empirical correction for the round-jet/plane-jet anomaly first proposed by Rodi [47]. The buoyancy term in the modelled ε-equation was empirical in nature and Hossain & Rodi [8] acknowledged that it would not be well suited to more general flow situations. To simulate the axisymmetric plume, they used a parabolic method where the numerical grid adjusted itself to the increase in plume width using a dimensionless stream function as a lateral coordinate. Both the limiting cases of pure jets and pure plumes were well predicted by the algebraic model as was the transition between jet and plume-behaviour in buoyant jets.

A number of more recent CFD simulations of axisymmetric buoyant plumes have also used variants of the standard $k - \varepsilon$ turbulence model. Nam & Bill [48] performed simulations of pool fires using the commercial code PHOENICS and modified the standard Launder & Spalding [49] model by changing, arbitrarily, the values of the effective Prandtl number, σ_{eff}, and the model constant, c_μ, from 1.0 and 0.09 to 0.614 and 0.109, respectively, to obtain improved results in buoyant plumes. They then used their modified model to simulate buoyant ceiling jets and found results to be slightly better than with the standard model. The consequences of changing these constants on the model's performance in other flows was not explored.

Hara & Kato [50] used a standard $k - \varepsilon$ model and presented results using different meshes with various modifications to the $c_{\varepsilon 3}$ constant in the buoyancy production term of the ε-equation. They compared results to the experiments of Yokoi [51], which involved releases of buoyant fluid through a circular orifice, but modelled this as a square orifice to enable the use of hexahedral Cartesian grids. Results were found to be grid-sensitive and recommendations regarding resolution

were provided. Differences in the $c_{\varepsilon 3}$ constant were found to have no effect on results.

The study by Brescianini & Delichatsios [42] also examined the $k - \varepsilon$ model in combination with different sub-models for the turbulence production due to buoyancy, including the Boussinesq Simple Gradient Diffusion Hypothesis (SGDH), the Generalized Gradient Diffusion Hypothesis (GGDH) of Daly & Harlow [52] and the algebraic model of Hossain & Rodi [8]. The SGDH and GGDH models are described in detail later in this UFR. They compared CFD predictions mainly to the experimental measurements of Dai *et al*. [41] and examined both axisymmetric and plane plumes. None of the model variants were found to capture all the flow details of both axisymmetric and plane plumes and no firm conclusions were drawn regarding the best turbulence buoyancy production model. The GGDH model was found to give improved predictions of the streamwise mass flux compared to SGDH. The Hossain & Rodi [8] model was also found sometimes to produce better results than GGDH. However, Brescianini & Delichatsios [42] noted that the Hossain & Rodi [8] model was sensitive to the model constants and was more complex to implement. They concluded that given the overall satisfactory performance of the $k - \varepsilon$ model in predicting the mean-flow quantities, there was no real advantage to be gained in using a higher-order closure model to study buoyant plumes.

Yan & Holmstedt [53] compared two $k - \varepsilon$ model variants against the George *et al*. [3] experiments for the axisymmetric plume. The first variant was a standard $k - \varepsilon$ model with SGDH and the second involved an additional algebraic stress model for the production term in the k-equation combined with GGDH for the production due to buoyancy. The additional algebraic stress model was based on a second-moment-closure correction devised by Davidson [54]. The standard $k - \varepsilon$ model with SGDH was found to underpredict the spreading rate of the plume, producing overly-high temperatures and velocities in the core. Their modified model produced better results for the axisymmetric plume. They went on to examine buoyant diffusion flames using their new approach.

Malin & Younis [55] also compared CFD predictions to the George *et al*. [3] data but used second-moment-closure models and the parabolic PHOENICS solver. The objective of Malin & Younis's study was to extend the second-moment closure model of Gibson & Younis [56][57][58] to buoyant flows and examine its performance in free turbulent jets and plumes. The model produced good predictions of the mean axial velocity and temperature profiles and was able to capture, at least qualitatively, the anisotropy in the Reynolds stresses.

Van Maele & Merci [2] recently examined both an axisymmetric and a plane buoyant wall plume using SGDH and GGDH variants of the standard $k - \varepsilon$ model and a realizable $k - \varepsilon$ model with the commercial code, Fluent. The SGDH source term was shown to have little effect in the axisymmetric plume case, and consequently the turbulent kinetic energy was underpredicted and the centreline velocity and temperature were overpredicted. The GGDH model was found to perform well with either of the two $k - \varepsilon$ model variants. For the axisymmetric plume case, results were compared to the experimental data of George *et al*. [3].

Finally, Craft *et al*. [59] mentioned briefly the results for the buoyant plume in discussing developments of their Two-Component Limit (TCL) second-moment-closure model. Predictions using the TCL model were compared to the experiments of Cresswell *et al*. [60] and results from a "basic" second-moment-closure model. The spreading rate of the self-similar buoyant plume was found to be better predicted using the more sophisticated TCL model.

Parabolic Solvers

A number of the early CFD studies discussed above used a parabolic or space-marching solution method. This involves the solution of simplified boundary-layer-type transport equations. Comparisons of model predictions using parabolic and elliptic codes for jets and plumes are given El Baz *et al*. [61], Magi *et al.* [62] and Haroutunian & Launder [63]. In axisymmetric free-jets, El Baz *et al*. [61] and Magi *et al.* [62] found that the use of an elliptic instead of a parabolic approach resulted in differences in the predicted spreading rates of 10% or more. In axisymmetric buoyant plumes, Haroutunian & Launder [63] found that spreading rates differed by only a few percent, but second moments differed by more than 30% in some cases. Given the capabilities of current desktop computers, there is no longer a need on the grounds of grid-resolution and computing time to use a parabolic solver in far-field plume simulations. However, care must be taken when using elliptic codes to ensure that the solution is not restricted or influenced by the side entrainment boundaries.

1.2.2 Studies on which this UFR review will be based

The work of Van Maele & Merci [2] has been chosen as providing the most appropriate currently available information on which comparisons have been made between CFD and experiment. Their study represents a good match for what is required for this UFR. They examined SGDH and GGDH variants of the both the standard $k - \varepsilon$ model and a realizable $k - \varepsilon$ model using the commercial CFD software, Fluent. The paper provides a thorough description of methodology used, including description of the numerical methods and a grid-dependence study. Both axisymmetric and plane wall plumes were examined, the former using the experimental data of George *et al*. [3]. The methodology used in their studies is described below.

2 Test Case

2.1 Brief Description of the Study Test Case

- Heated air is discharged through a circular orifice into ambient air that is at rest.
- The plume source temperature is 300°C and the ambient air is 29°C.
- The source has diameter, $D = 6.35$ cm.
- The hot air is discharged at a velocity of $U_0 = 67$ cm/s with a approximately a top-hat profile.
- Temperature and velocity fluctuations at the inlet are less than 0.1%.
- George *et al*. [3] presented experimentally measured profiles of both mean and fluctuating components of the temperature and axial velocity in the self-similar region at $x/D = 8$, 12 and 16 above the source.

2.2 Test Case Experiments

The experiments used in this UFR are those of George *et al*. [3] which were conducted in 1974 at the Factory Mutual Research Corporation and were subsequently repeated by Shabbir & George [34] at the University of Buffalo.

The general arrangement is shown in Figure 4. Compressed air is passed through a set of heaters and porous mesh screens before exiting through a nozzle into the enclosure. The nozzle is stated as a 15:1 contraction in [3], a 12:1 contraction in [34] and appears to be different again in a drawing of the arrangement in [3] (see Figure 5). It resulted in a velocity profile through the exit which was uniform to within 2% outside the wall boundary layer. The velocity and temperature fluctuations at the exit were measured to be very low, less than 0.1% in [3] and 0.5% in [34]. The temperature of the source was 300°C and the ambient environment 29°C. Both were controlled to an accuracy of within 1°C. The discharge velocity was 67 cm/s, as calculated from the measured heat flux. These source conditions corresponded to Reynolds number, $Re_0 = 870$, and densimetric Froude number, $Fr_0 = 1.23$[3]. There was no evidence of laminar flow behaviour at a position two inlet diameters downstream from the source. The effective origin of the plume, x_0, was found to be at the same location as the exit (see [3] for details of how this was determined).

The screen enclosure around the plume exit was 2.44 × 2.44 metres in cross-section and 2.44 metres high (there is, presumably, an error in [3] which suggests that the enclosure is 2.44 × 2.44 × 2.44 mm). In the later Shabbir & George experiments, a 2 × 2 × 5 metre enclosure was used. The purpose of the screens was to minimize the effect of cross-draughts and other disturbances affecting the flow. Two-wire probes were used by George *et al*. [3] to record velocities and temperature.

3 The densimetric Froude number is calculated here from the source and ambient temperatures, the exit velocity and source diameter given by George *et al*. [3], using Equation (1). However, George *et al*. [3] stated that the densimetric Froude number was 1.4. It is unclear how they determined this value. Using the approach taken by Chen & Rodi [1] in which the source density instead of the ambient density is used to make the density difference dimensionless, and Froude number is defined using the square of the expression given in Equation (1), this gives a Froude number of 0.80.

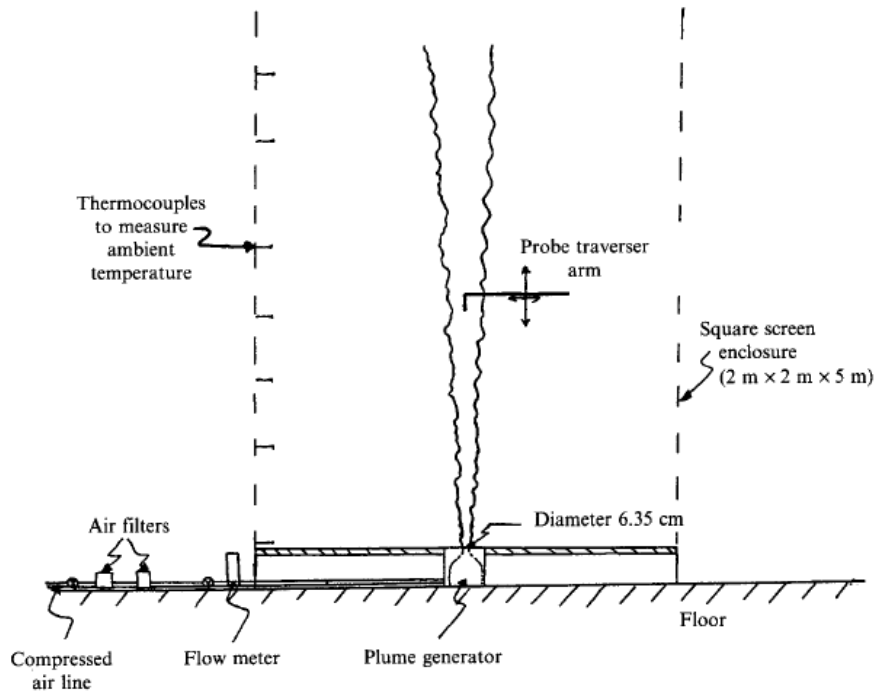

Figure 5 Schematic of the George *et al*. [3] experiments, from Shabbir & George [11].

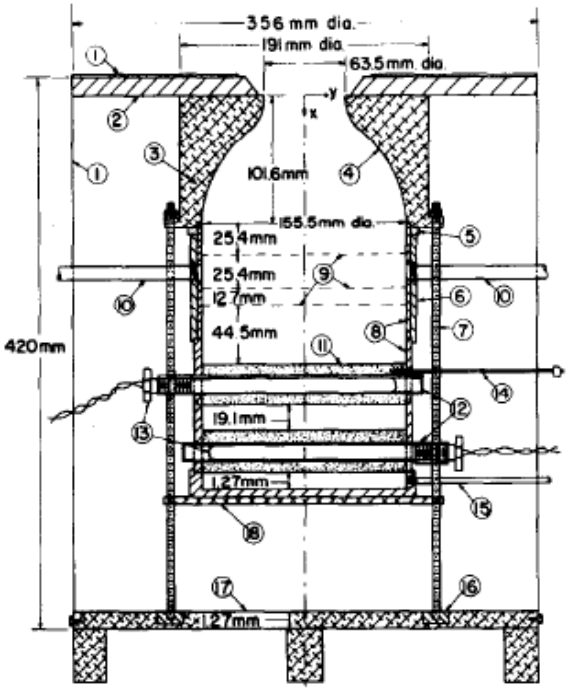

FIG. 2. Schematic of thermal plume generator.
(1) Container for silica aerogel insulation, sheet steel. (2) Cerafelt insulation; 1.27 mm thick. (3) Aluminum exit nozzle. (4) Inner aluminum surface machined approximately to:

Figure 6 Schematic of the plume generator used in the experiments, from George *et al*. [3].

George *et al*. [3] reported that measurement errors, stemming from directional ambiguity of the hot wire and its thermal inertia, were around 3% for the velocity and lower for other mean and RMS values. The frequency response of the hot wires was estimated to be around 300 Hz compared to the frequency of the energy-containing eddies at around 50 Hz and the Kolmogorov microscale at 1 Khz. It was noted that measurement errors were likely to be higher on the outer edge of the plume were the velocity fluctuations were higher.

In their review of plume experiments, Chen & Rodi [1] noted that the data from George *et al.* differed significantly from earlier measurements by Rouse *et al*. [64]. However, they considered it to be more reliable due to its use of more sophisticated instrumentation. George [40], describes an experimental program at the University of Buffalo that was set up following publication of the original George *et al.* [3] paper to investigate possible causes of differences in experimental plume results. Possible sources of errors discussed included:

- ambient thermal stratification
- the size of the enclosure
- the use of porous screens used to minimise disturbances from the far-field affected the plume source.
- hot wire measurement errors

The most significant concern was ambient thermal stratification. One of the features of buoyant plumes in neutral environments is that the integral of the buoyancy across the whole cross-section of the plume, F, should remain constant and equal to the buoyancy added at the source, F_0. George [40] discussed how thermal stratification involving small temperature differences of the order of 1°C across a 3 metre vertical span would be sufficient to cause F to decrease to only 50% of the source value. This would be likely to cause differences in measured temperature and velocity plume profiles.

In the initial experiments of George *et al*. [3], the thermal stratification was not strictly controlled. However, results from later experiments published in the PhD thesis of Shabbir [32] (reproduced in [34] and [40]), which conserved buoyancy to within 10%, are in good agreement with the earlier results from George *et al*. [3]. This suggests that, perhaps fortunately, ambient thermal stratification did not contaminate the George *et al*. [3] results significantly.

A summary of the original results from George *et al*. [3] and those reproduced later by Shabbir & George [11] is presented in Table 3. Also shown are the recommended values from Chen & Rodi's review [1] and other studies. The parameters given in Table 3 relate to the following empirical formulae for the mean vertical velocity:

$$W = F_0^{-1/3} z^{-1/3} f_w \tag{9}$$

and effective buoyancy acceleration:

$$g\frac{\Delta\rho}{\rho} = F_0^{2/3} z^{-5/3} f_T \tag{10}$$

where f_w and f_T are Gaussian functions:

$$f_w = A_w \exp\left[-B_w\left(\frac{r}{x}\right)^2\right] \qquad f_T = A_T \exp\left[-B_T\left(\frac{r}{x}\right)^2\right] \tag{11}$$

The parameters, $l_{\Delta T/2}$ and $l_{w/2}$ are the dimensionless half-widths of the plume, as defined by the

location where the normalized buoyancy or mean velocity falls to half its centreline value. The RMS temperature and axial velocity fluctuations normalized by the centreline mean values are denoted, $\left(\overline{t^2}\right)^{1/2}/\Delta T_c$ and $\left(\overline{w^2}\right)^{1/2}/W_c$, respectively.

As noted earlier, Dai *et al*. [10][37][38][39][41] disputed the accuracy of the George *et al*. [3] experiments and suggested that they had made measurements too near the source, before the plume had reach a fully-developed state. Their arguments are disregarded by Shabbir & George [11][34].

Table 3 Summary of mean flow parameters and turbulence intensities, from Shabbir & George [11]

Reference	A_T	A_W	B_T	B_W	$l_{\Delta T/2}$	$l_{W/2}$	$(\overline{t^2})^{1/2}/\Delta T_c$	$(\overline{w^2})^{1/2}/W_c$
Rouse *et al.*	11.0	4.7	71	96	0.095	0.084	—	—
George *et al.*	9.1	3.4	65	55	0.104	0.112	0.38	0.28
Nakagoma & Hirata	11.5	3.89	48.1	63	0.105	0.12	0.36	0.25
Papanicolaou & List	14.28	3.85	80	90	0.093	0.0877	0.42	0.25
Chen & Rodi	9.35	3.5	65	55	0.10	0.112	—	—
Present study	9.4	3.4	68	58	0.10	0.107	0.40	0.33

TABLE 2. Summary of mean flow parameters and turbulence intensities

2.3 CFD Methods

2.4 Van Maele & Merci: Description of CFD Work

2.4.1 Numerical Methods

Van Maele & Merci [2] used the finite-volume-based commercial CFD code, Fluent[4], to simulate the plume experiments of George et al. [3]. For the discretization of the convective terms in the momentum, turbulence and energy equations a second-order upwind scheme was used. Diffusion terms were discretized using second-order central differences and the SIMPLE algorithm was used for pressure-velocity coupling. The flow was treated as axisymmetric and elliptic calculations were performed used a Cartesian grid arrangement.

The low-Mach-number form of the Favre-averaged Navier-Stokes equations were used. In this weakly-compressible approach, the density is treated as only a function of temperature and not pressure. Pressure only affects the flow field through the pressure-gradient term in the momentum equations. The ideal gas law is used to link the mean density, $\overline{\rho}$, to mean temperature, T as follows:

$$p_* = \overline{\rho} R T \tag{12}$$

where p_* is taken as constant and equal to the atmospheric pressure. The low-Mach-number approximation implies that the effect of the mean kinetic energy and the work done by viscous stresses and pressure are negligible in the energy equation.

4 http://www.fluent.com

2.4.2 Turbulence Modelling

Two turbulence models were used by Van Maele & Merci [2]: the standard $k - \varepsilon$ model of Jones & Launder [65] and the realizable $k - \varepsilon$ model of Shih *et al*. [66]. In the former model, the eddy viscosity is given by:

$$\mu = \overline{\rho}\, c_\mu \frac{k^2}{\varepsilon} \tag{13}$$

where c_μ is a constant equal to 0.09 and the standard k and ε equations are written:

$$\frac{\partial}{\partial x_j}\left(\overline{\rho}\, U_j k\right) = \frac{\partial}{\partial x_j}\left[\left(\mu + \frac{\mu}{\sigma_k}\right)\frac{\partial k}{\partial x_j}\right] + P_k + G - \overline{\rho}\,\varepsilon \tag{14}$$

$$\frac{\partial}{\partial x_j}\left(\overline{\rho}\, U_j \varepsilon\right) = \frac{\partial}{\partial x_j}\left[\left(\mu + \frac{\mu}{\sigma_\varepsilon}\right)\frac{\partial \varepsilon}{\partial x_j}\right] + c_{\varepsilon 1} P_k \frac{\varepsilon}{k} - c_{\varepsilon 2}\overline{\rho}\frac{\varepsilon^2}{k} + S_{\varepsilon B} \tag{15}$$

where $c_{\varepsilon 1} = 1.44$, $c_{\varepsilon 2} = 1.92$, $\sigma_k = 1.0$, $\sigma_\varepsilon = 1.3$ and P_k is the production term due to mean shear. The terms G and $S_{\varepsilon B}$ are source terms related to the influence of buoyancy on the k and ε equations. The treatment of these terms is discussed below.

The Shih *et al*. [66] model involves two changes to standard $k - \varepsilon$ model. Firstly, c_μ is made a function of strain and vorticity invariants to ensure that the model always returns positive normal Reynolds stresses and satisfies the Schwarz inequality for the turbulent shear stresses. The function form of c_μ is given by:

$$c_\mu = \left(A_0 + A_s U^{(*)} \frac{k}{\varepsilon}\right)^{-1} \tag{16}$$

where:

$$U^{(*)} = \sqrt{S_{ij} S_{ij} + \Omega_{ij}\,\Omega_{ij}} \qquad S_{ij} = \frac{1}{2}\left(\frac{\partial U_i}{\partial x_j} + \frac{\partial U_j}{\partial x_i}\right) \qquad \Omega_{ij} = \frac{1}{2}\left(\frac{\partial U_i}{\partial x_j} - \frac{\partial U_j}{\partial x_i}\right) \tag{17}$$

$$A_s = \sqrt{6}\cos\phi \qquad \phi = \frac{1}{3}\arccos\left(\sqrt{6}\,W\right) \qquad W = 2^{3/2}\frac{S_{ij} S_{jk} S_{ki}}{S^3} \qquad S = \sqrt{2 S_{ij} S_{ij}} \tag{18}$$

and A_0 is a constant equal to 4.04.

Secondly, a different ε-equation is used in to resolve the problem of the round-jet/plane-jet anomaly (see Pope [67]):

$$\frac{\partial}{\partial x_j}\left(\overline{\rho}\, U_j \varepsilon\right) = \frac{\partial}{\partial x_j}\left[\left(\mu + \frac{\mu}{\sigma_\varepsilon}\right)\frac{\partial \varepsilon}{\partial x_j}\right] + c_{\varepsilon 1}\overline{\rho}\, S \frac{\varepsilon}{k} - c_{\varepsilon 2}\overline{\rho}\frac{\varepsilon^2}{k + \sqrt{\nu\,\varepsilon}} + S_{\varepsilon B} \tag{19}$$

$$c_{\varepsilon 1} = max\left[0.43, \eta/(\eta + 5)\right] \qquad \eta = S\,k/\varepsilon \tag{20}$$

where S is the strain-rate invariant as before, $c_{\varepsilon 2} = 1.9$, $\sigma_k = 1.0$ and $\sigma_\varepsilon = 1.3$.

The Shih *et al*. [66] model was developed for high Reynolds number turbulent flows and therefore a zonal or wall-function approach must be used to bridge the viscous sub-layer near walls. Compared to the standard $k - \varepsilon$ model, it has been shown to produce improved behaviour in a number of free shear flows, boundary-layer flows and a backward-facing step flow [66]. One of the major

weaknesses of the standard $k-\varepsilon$ model is that it produces too much turbulent kinetic energy at stagnation points [68]. The Shih *et al.* model should in principle suffer less from this weakness since the functional form of c_μ should reduce the over-production of k. However, its overall performance in stagnating flows will depend on the type of wall model used.

Production due to Buoyancy, *G*

The term G in the k-equation relates to the influence of buoyancy on the turbulent kinetic energy, and is given by:

$$G = \overline{\rho u_j} g_j \tag{21}$$

where g_j is the gravitational acceleration vector. In stably stratified flows, where the temperature increases with height, G is negative. Conversely, in unstably stratified flows, where temperature decreases with height, G is positive and acts to increase k. The unknown density-velocity correlation, $\overline{\rho u_j}$, must be modelled. The most common approximation of this term is the so-called Boussinesq Simple Gradient Diffusion Hypothesis (SGDH):

$$\overline{\rho u_j} = -\frac{\mu_t}{\sigma_t}\frac{1}{\overline{\rho}}\frac{\partial \overline{\rho}}{\partial x_j} \tag{22}$$

The production due to buoyancy using SGDH is then as follows:

$$G = -\frac{\mu_t}{\sigma_t}\frac{1}{\overline{\rho}^2}\frac{\partial \overline{\rho}}{\partial x_j}\rho_\infty g_j \tag{23}$$

In their paper, Van Maele & Merci [2] erroneously included an additional pressure-gradient term $\left(\partial P/\partial x_j\right)$ in Equation (23) related to the pressure-work rather than buoyancy (see Wilcox [69]). Since the term is negligible in incompressible flows, such as the buoyant plumes considered here, it has therefore been ignored. The ratio of the reference density to the mean density, $\rho_\infty/\overline{\rho}$, appears in Equation (23) due to the use of a non-Boussinesq approach and Favre-averaging, which are discussed later. Van Maele & Merci [2] assumed that σ_t was constant and equal to 0.85.

Instead of writing the buoyancy production in terms of the density-velocity correlation, $\overline{\rho u_j}$, the equation can be written in terms of the heat flux, $\overline{u_j t'}$:

$$\overline{u_j t'} = -\frac{\mu_t}{\sigma_t}\frac{\partial T}{\partial x_j} \tag{24}$$

and the G term is then written:

$$G = -\beta\frac{\mu_t}{\sigma_t}\frac{\partial T}{\partial x_j} g_j \tag{25}$$

where t' is the temperature fluctuation, T is the mean temperature and β is the volumetric expansion coefficient, $\beta = -\left(1/\overline{\rho}\right)\partial\overline{\rho}/\partial T$. Other equivalent expressions can also be formulated using the ideal gas law and the assumption that density is only a function of temperature, not pressure (the low-Mach-number approximation). The conversion from mean density to temperature gradients is then as follows:

$$\frac{\partial \overline{\rho}}{\partial x_j} = \frac{\partial \overline{\rho}}{\partial T}\frac{\partial T}{\partial x_j} = \frac{-P_*}{RT^2}\frac{\partial T}{\partial x_j} = \frac{\overline{\rho}}{T}\frac{\partial T}{\partial x_j} \tag{26}$$

The SGDH model predicts zero density-velocity correlation or heat flux components ($\overline{\rho u_j} = 0$ or $\overline{u_j t'} = 0$) in situations were the density or temperature gradients are zero in that direction. However, as Ince & Launder [70] noted, in a simple shear flow in which there are only cross-stream temperature gradients, the heat flux in the streamwise direction actually exceeds that in the cross-stream direction. This shortcoming of the SGDH model was confirmed by the analysis of Shabbir & Taulbee [33], who showed that the model significantly underestimates the magnitude of the heat flux in vertical buoyant plumes. The underprediction of $\overline{\rho u_j}$ or $\overline{u_j t'}$ by the SGDH model leads to an overly-small production term, G, and hence a turbulent kinetic energy, k, which is too small, producing too little mixing in the modelled plume. The study by Yan & Holmstedt [53] provides a clear example of how the $k - \varepsilon$ model with SGDH produces buoyant plumes which are too narrow and with overly high temperatures and velocities in the core of the flow.

Van Maele & Merci [2] examined a different model for G based on the the Generalized-Gradient Diffusion Hypothesis (GGDH) of Daly & Harlow [52]. This was first used in the context of practical CFD calculations with the $k - \varepsilon$ model by Ince & Launder [70], and is written as follows:

$$\overline{\rho u_j} = -\frac{3}{2}\frac{c_\mu}{\sigma_t}\frac{k}{\varepsilon}\left(\overline{u_j u_k}\frac{\partial \overline{\rho}}{\partial x_k}\right) \tag{27}$$

which Van Maele & Merci [2] expressed as follows:

$$G = -\frac{3}{2}\frac{\mu_t}{\sigma_t \overline{\rho}^2 k}\left(\overline{u_j u_k}\frac{\partial \overline{\rho}}{\partial x_k}\right)\rho_\infty g_j \tag{28}$$

again with σ_t = 0.85. As previously, Van Maele & Merci [2] included a pressure-gradient term in the above equation related to pressure-work but this can effectively be ignored in the present application. The advantage of the GGDH approach is that transverse density gradients affect the production term.

In their plume simulations, Van Maele & Merci [2] used a slightly modified form of the above relation. They replaced the normal stress in the streamwise (vertical) direction, $\overline{ww}$, with the turbulent kinetic energy, k. They justified this on the basis that the $k - \varepsilon$ model gives poor predictions of normal stresses in plumes. Experimental measurements indicate that the streamwise normal stress is approximately twice the magnitude of the transverse components (i.e. $\overline{ww} \approx 2\,\overline{uu}$) whereas the $k - \varepsilon$ model predicts them to be roughly equal. Since k can be approximated from $k \approx \frac{1}{2}\left(\overline{ww} + 2\,\overline{uu}\right)$ and the $k - \varepsilon$ model predicts $\overline{ww} \approx \overline{uu}$, they suggest that it is more appropriate to use k rather than $\overline{ww}$, to artificially increase the stress to a more realistic value. This ad-hoc correction may not be appropriate in more complex flows where the gravitational vector is not aligned to the Cartesian axes.

A simplification frequently made to the buoyancy treatments described above is to assume that the mean density is equal to the reference density, $\overline{\rho} \approx \rho_\infty$, an approach known as the Boussinesq approximation[5]. For the SGDH written in terms of temperature gradients, this gives:

5 A more complete definition of the Boussinesq approximation is that the variation in fluid properties due to changes in temperature or pressure are assumed to be zero (i.e. not only constant density, but constant molecular viscosity,

$$G = -\beta \frac{\mu_t}{\sigma_t} \frac{\partial T}{\partial x_j} g_j \tag{29}$$

Van Maele & Merci [2] examined the effect of this simplification on the prediction of the George *et al*. [3] buoyant plume experiments .

Buoyancy Source Term in the ε-Equation, $S_{\varepsilon B}$

The buoyancy source term, $S_{\varepsilon B}$, in the ε-*e*quation is given by:

$$S_{\varepsilon B} = c_{\varepsilon 1}\left(1 - c_{\varepsilon 3}\right)\frac{\varepsilon}{k} G \tag{30}$$

Unlike other model constants in the $k - \varepsilon$ model, there is still some controversy over the best value or formula for $c_{\varepsilon 3}$. Different approaches have been proposed by different researchers, partly depending on whether the flows are horizontal or vertical and whether there is stable or unstable stratification. For a review of the performance of various models, see Rodi [71], Markatos *et al*. [72] or Worthy *et al*. [73]. In their paper, Van Maele & Merci [2] provided a summary of the values proposed previously in 20 published papers and, based on analysis of these studies, used a constant value for $c_{\varepsilon 3}$ of 0.8.

Favre-Averaging

Throughout their paper, Van Maele & Merci [2] refer to Favre-averaged mean velocity, enthalpy and temperature ($\widetilde{U}$, $\tilde{h}$ and $\widetilde{T}$) instead of the perhaps more familiar Reynolds-averaged values, (*U*, *H* and *T*). The Favre average of a variable ϕ , denoted $\tilde{\phi}$ is calculated from:

$$\tilde{\phi} = \frac{\overline{\rho \phi}}{\overline{\rho}} \tag{31}$$

where overbars represent long time or ensemble averages in the traditional Reynolds-averaged sense. The turbulent stresses appearing in the Favre-averaged Navier-Stokes equations are:

$$-\widetilde{u_i u_j} = 2 \nu_t \widetilde{S}_{ij} - \frac{2}{3} k \delta_{ij} \tag{32}$$

This is the same as the usual Reynolds-averaged stress except that the strain-rate tensor, $\widetilde{S}_{ij}$ is now Favre-averaged. The Favre-averaged strain-rate is calculated from:

$$\widetilde{S}_{ij} = \frac{1}{2}\left(\frac{\partial \widetilde{U}_i}{\partial x_j} + \frac{\partial \widetilde{U}_j}{\partial x_i}\right) \tag{33}$$

where the Favre-averaged mean velocity, $\widetilde{U}_i$, is the parameter solved for in the momentum

thermal conductivity etc.). In Van Maele & Merci's work, although they stated that they tested the Boussinesq approximation, in fact their simplifications only consisted of assuming $\overline{\rho} \approx \rho_\infty$ in the production term, *G* (Van Maele, private communication, 2007). It is unclear whether variation of the density in the other remaining terms, or variation of the viscosity, thermal conductivity etc., affected the results significantly.

equations.

Even though they solved Favre-averaged transport equations, Van Maele & Merci modelled the buoyancy production term, G, using the Reynolds-averaged stress, not the Favre-averaged stress. Formally, one can expand the Reynolds-averaged stress as follows [74]:

$$\overline{u_i u_j} = \widetilde{u_i u_j} - \frac{\overline{\rho u_i u_j}}{\overline{\rho}} - \frac{\overline{\rho u_i}\,\overline{\rho u_j}}{\overline{\rho}^2} \tag{34}$$

However, it is often assumed that the last two terms in this expansion can be neglected, in which case $\overline{u_i u_j} \approx \widetilde{u_i u_j}$. This was the approach adopted by Van Maele & Merci [2].

If one replaces all the Favre-averaged quantities in Van Maele & Merci's equations with Reynolds-averaged quantities (i.e. substitute ~ symbols with –), their equations appear identical to the incompressible Reynolds-averaged Navier-Stokes equations. In terms of the actual coding of the model, the mean quantities in the flow equations can therefore be interpreted as either Reynolds-averaged or Favre-averaged variables. For this reason, the transport equations have been written in this UFR without the Favre-averaged (~) symbols.

In the majority of the other papers reviewed for this UFR, the transport equations are stated as being Reynolds averaged. Hossain & Rodi [8] noted that correlations between fluctuating velocities and fluctuating density are important in combustion applications but are small in comparison to correlations between velocity fluctuations in simple buoyant plumes. Brescianini & Delichatsios [42] also commented that "depending on certain assumptions, the mean quantities ... can be interpreted as either time-averaged or Favre-averaged variables. The differences between these two types of averages is small when compared to the experimental uncertainties for the plumes examined in this study, and as a result, no large distinction is made between the two forms". In the experiments of O'Hern *et al*. [75], reviewed for the companion UFR on unsteady plumes, simultaneous measurements were made of velocities and mass fraction. This enabled both Favre-averaged and Reynolds-averaged quantities to be derived. O'Hern *et al*. [75] found that the difference between Favre- and Reynolds-averaged velocities and second-order turbulent statistics was less than the uncertainty in the data throughout the flow field. Further details on Favre-averaging can be found in Chassaing *et al*. [74].

2.4.3 Boundary Conditions

Van Maele & Merci [2] modelled the plume source using a diameter, D_0 , of 6.35 cm, an inlet temperature of 573 K, an axial velocity of 0.67 m/s, and a turbulence intensity of 0.5% . To define a value for ε at the inlet, they assumed a turbulence length scale $(k^{3/2}/\varepsilon)$ of 4.5 mm, equivalent to $D_0/15$. Around the source, on the radial plane, a wall boundary was specified. The domain was axisymmetric, extending 1 metre in the radial direction and 3 metres in the axial direction. On the side and top boundaries, static pressure conditions were specified to allow the flow into or out of the computational domain. Ambient air entrained through the open boundaries was assumed to have a temperature of 302 K, a turbulent kinetic energy of 10^{-6} m^2/s^2 and a dissipation rate of 10^{-9} m^2/s^3. The atmospheric pressure was taken as 101 325 Pa. No tests were undertaken to examine whether the location or conditions of the entrainment boundaries affected the flow solution.

2.4.4 Grid Used

Van Maele & Merci [2] used a 40 × 100 node rectangular grid in the (radial × axial) directions. There were 10 equispaced cells across the source and 30 across the adjacent wall region. The grid was stretched in both the axial and radial directions from the source.

To ensure that results were grid-independent, Van Maele & Merci performed simulations using 80 × 200 and 160 × 400 node grids. The predicted spreading rates and centreline values on the coarsest and finest grids differed by less than 2%. The 40 × 100 grid was therefore considered to provide adequately grid-independent results.

2.4.5 Discussion

The CFD methodology employed by Van Maele & Merci appears to have been performed to a high standard. Details of the modelling and numerical techniques used in their work were recorded clearly in their paper.

They did not show a plot of the grid that was used, however this may have been because it would not have been well reproduced in print and, in any case, the mesh was a simple Cartesian grid arrangement and is adequately described in the text.

The sensitivity of results to the turbulence length scale at the inlet, and to the level of turbulence in the entrained air was not explored, although reasonable approximations appear to have been used for these values. Likewise, the sensitivity to the size of the domain and the entrainment boundaries was not explored.

3 Evaluation

3.1 Comparison of CFD Calculations with Experiments

Van Maele & Merci [2] presented the results from a number of simulations that examined the effects of different combinations of models and approximations. The Boussinesq approximation $(\overline{\rho} \approx \rho_\infty)$ was shown to have no affect on the model predictions when the SGDH model was used. Indeed, the SGDH source term itself had a negligible influence on the results. When using the GGDH source term, however, the Boussinesq approximation had an effect on the results nearest to the plume exit at z/D = 12, where the assumption of $(\overline{\rho} \approx \rho_\infty)$ caused an increase in the peak velocity of around 5%. By assuming that the mean density was the same as the reference density, the buoyancy source term became smaller and so the turbulent kinetic energy and hence the eddy viscosity were also smaller. As a consequence, there was less mixing, the centreline velocity increased and the spreading rate decreased. The effect was significant where the mean density differed most from the reference density, nearest to the plume source, but was negligible in the far field. These results suggest that the Boussinesq approximation can be used in the far field of buoyant plumes where density differences are small. However, if the CFD domain extends from the far field to the source of buoyancy, such as a fire or strongly heated surface where density differences are appreciable, then the Boussinesq approximation should not be used.

It should also be remembered that Van Maele & Merci's interpretation of the 'Boussineq approximation' only involved setting $(\overline{\rho} \approx \rho_\infty)$ in the production term, G. The density and other flow properties (molecular viscosity, specific heat etc.) still varied as a function of temperature elsewhere in the transport equations.

Van Maele & Merci examined the effects of SGDH versus GGDH and the effect of switching on and off both the production due to buoyancy term, G, and the source term in the ε-equation, $S_{\varepsilon B}$, on the standard and realizable $k-\varepsilon$ models. Table 4 summarizes the cases tested. In the relevant cases, they used the full buoyancy source term G rather than any truncated form of the equation. The ε-equations were different for standard and realizable models, but in both cases, where used, the buoyancy-related source term was given by:

$$S_{\varepsilon B} = c_{\varepsilon 1}\left(1 - c_{\varepsilon 3}\right)\frac{\varepsilon}{k}G \qquad \text{with} \qquad c_{\varepsilon 3} = 0.8 \tag{35}$$

The results were compared to the experimental data of George *et al.* [3] and the correlations of Shabbir & George [11], which were given by:

Axial velocity:
$$W F_0^{-1/3} z^{1/3} = 3.4 \exp\left(-58\eta^2\right) \tag{36}$$

Buoyancy:
$$g\beta\Delta T F_0^{-2/3} z^{5/3} = 9.4 \exp\left(-68\eta^2\right) \tag{37}$$

where W is the mean axial momentum, ΔT is the difference between the local mean and ambient temperatures, z is the vertical distance from the source, $\eta = r/z$ is the similarity variable (r is the radial distance from the plume centreline), and β the thermal expansion coefficient. The buoyancy added at the source, F_0, is found from :

$$F_0 = 2\pi \int_0^{r_0} W g \frac{\delta \rho}{\rho_\infty} r \, \mathrm{d}r \tag{38}$$

and was 1.0×10^{-6} cm^4/s^3 in the George *et al*. plume [3]. To compare to these empirical correlations, Van Maele & Merci used their results taken at a position, z = 1.75 m, equivalent to approximately 28 inlet diameters from the source. To demonstrate that this was sufficiently far from the source to produce self-similar profiles, the dimensionless velocity and temperature profiles were shown to be practically identical at a distance of 2.75 m.

Profiles of the mean axial velocity and buoyancy are compared to the empirical correlations in Figures 7 and 8. A summary of the centreline values and spreading rates for velocity and temperature are given in Table 5. This shows the measured values from the experiments of George *et al*. [3], the recommended values given by Chen & Rodi [1] from their analysis of plume experiments up to 1980, the subsequent measured values from Shabbir & George [11], the RANS results from Van Maele & Merci [2] and Hossain & Rodi [8], and the LES results from Zhou *et al*. [28]. Three results are taken from Hossain & Rodi: Case A which is from a $k - \varepsilon$ model without any buoyancy modifications, Case B which is from a $k - \varepsilon$ model with buoyancy corrections in both k and ε equations, and Case C which is from Hossain & Rodi's algebraic stress/flux model.

For the Van Maele & Merci [2] results, both the standard and realizable $k - \varepsilon$ models without buoyancy modifications (cases SKE and RKE) predicted overly large centreline velocity and buoyancy values and under-predicted the spreading rates of the plume. When the SGDH source term was used, with or without $S_{\varepsilon B,}$, it had practically no effect on the results. This may have been partly due to the particular choice of the constant $c_{\varepsilon 3}$ which made the contribution from the buoyancy production small relatively to shear production in the ε-equation. The SKE, SKE_A and SKE_A* cases all returned very similar predictions to each other and RKE, RKE_A and RKE_A* cases behaved similarly. This was shown by Van Maele & Merci to be a consequence of the SGDH source term being negligible in comparison to other terms in the k and ε equations.

Table 5 shows that for the basic $k - \varepsilon$ model without any buoyancy corrections there are significant differences in terms of the predicted spreading rates between the results of Van Maele & Merci [2] and Hossain & Rodi [8] (cases SKE and A, respectively). Van Maele & Merci's predictions of the spreading rates are nearly 20% higher. This may have been due to the choice of non-standard model constants by Hossain & Rodi [8], who used $c_\mu = 0.109$ and $\sigma_t = 0.614$, whilst Van Maele & Merci [2] used $c_\mu = 0.09$ and $\sigma_t = 0.85$. The results for the $k - \varepsilon$ model with buoyancy corrections are more similar (Cases SKE_A and B, respectively). Here, in addition to the non-standard c_μ and σ_t constants, Hossain & Rodi [8] used a model with constant $c_{\varepsilon 3}$ scaled by the Richardson number, which was zero in the vertical buoyant plume, such that the buoyancy production had the same weight as the shear production.

Use of the GGDH model produced some improvements in the results presented by Van Maele & Merci [2]. For the SKE_B model, the centreline value was well-predicted but the half-width of the plume was overpredicted by around 20%. When the buoyancy source term in the ε-equation was omitted (case SKE_B*) the axial velocity on the centreline was reduced and the half-width prediction became even more inaccurate. This is consistent in the SKE_B* case with the turbulent kinetic energy being overpredicted due to the removal of a positive source in the ε-equation.

For the realizable model with GGDH, the mean axial velocity and buoyancy were over-predicted on the centreline by around 10% and 20% respectively but the half-width was reasonably close to the experimental values. Switching off the buoyancy-related source term in the ε-equation (case

RKE_B*) led to a slight improvement in the results, however Van Maele & Merci noted that this also reduced the numerical stability of the calculation. Details of any source-term linearisation used to improve robustness are not provided in their paper. They recommended that the $S_{\varepsilon B}$ term should be retained in the modelled equations to avoid convergence difficulties.

Van Maele & Merci commented that, overall, the GGDH variant of the realizable model (RKE_B) performed better than the equivalent standard $k - \varepsilon$ model (SKE_B). However, the standard model gave better peak mean axial velocity and buoyancy predictions (to within 2% and 10%, respectively, compared to 10% and 25% for the RKE_B model). It could also be argued that the realizable model only gives good predictions for the plume half-width because the predicted profiles happen to cross the experiment profiles at the correct position, the actual shape of the predicted profiles are incorrect. One could conclude, perhaps, that both standard and realizable models predict the axisymmetric plume to a similar overall level of accuracy. Neither provides an exact solution and the errors for the two models are slightly different.

Table 4 Summary of the model variants tested by Van Maele & Merci [2]

Case Ref.	*Turbulence Model*	*G*	$S_{\varepsilon B}$
SKE	Standard $k-\varepsilon$	-	-
SKE_A	Standard $k-\varepsilon$	SGDH	Eqn (35)
SKE_A*	Standard $k-\varepsilon$	SGDH	-
SKE_B	Standard $k-\varepsilon$	GGDH	Eqn (35)
SKE_B*	Standard $k-\varepsilon$	GGDH	-
RKE	Realizable $k-\varepsilon$	-	-
RKE_A	Realizable $k-\varepsilon$	SGDH	Eqn (35)
RKE_A*	Realizable $k-\varepsilon$	SGDH	-
RKE_B	Realizable $k-\varepsilon$	GGDH	Eqn (35)
RKE_B*	Realizable $k-\varepsilon$	GGDH	-

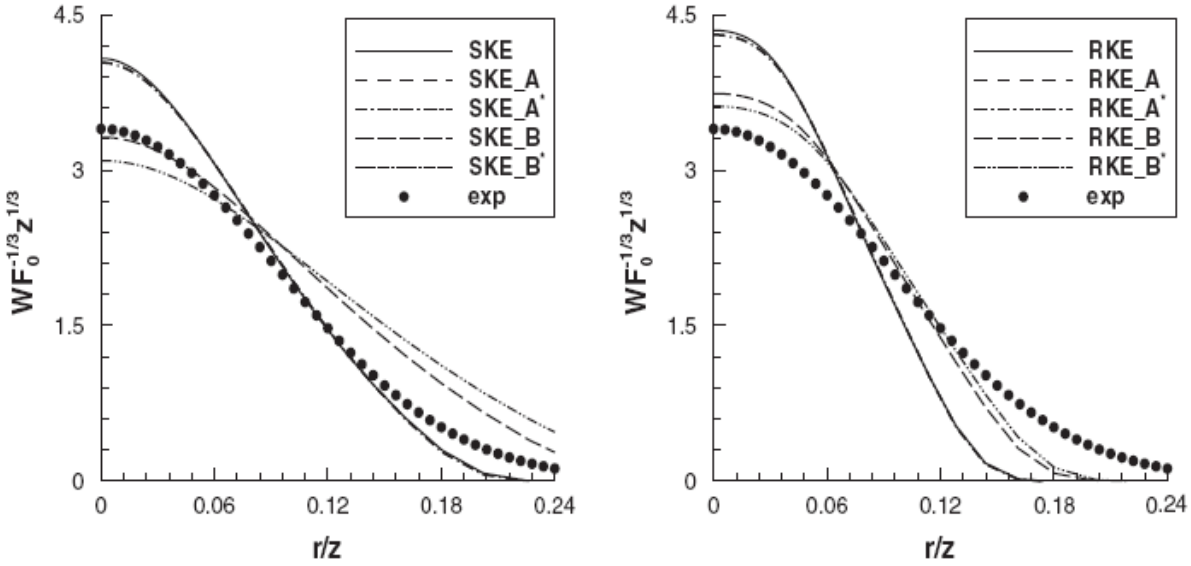

Figure 7 Mean axial velocity profiles expressed in terms of similarity variables, from Van Maele & Merci [2].

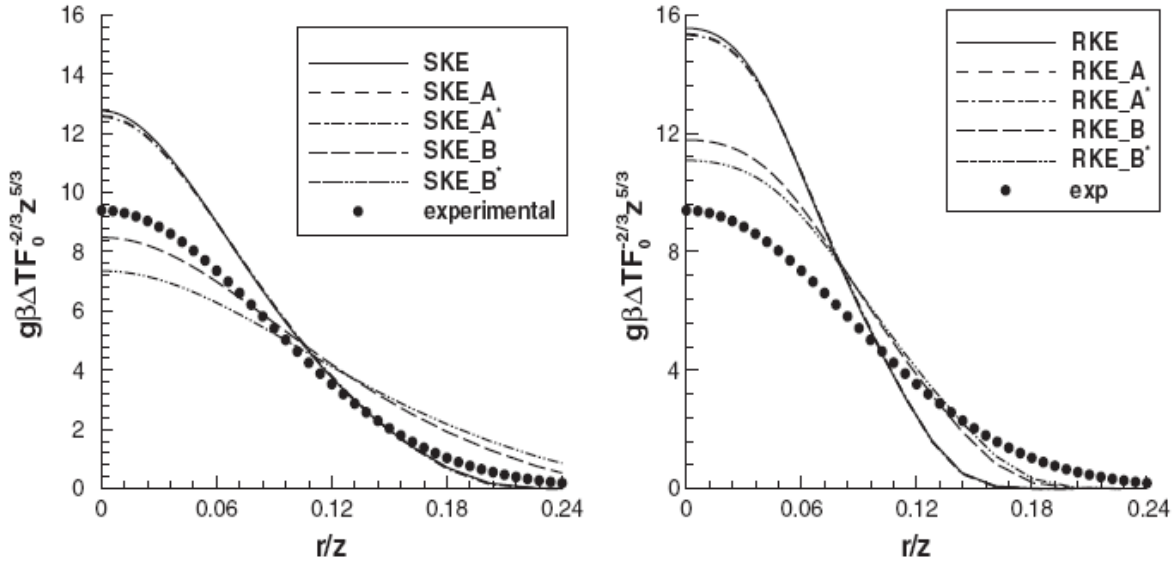

Figure 8 Mean buoyancy profiles expressed in terms of similarity variables, from Van Maele & Merci [2].

Table 5 Centreline values and half-widths of the plume in terms of mean axial velocity and buoyancy.

	$(W F_0^{-1/3} z^{1/3})_c$	$l_{W/2}$	$(g\beta\Lambda TF_0^{-2/3} z^{5/3})_c$	$l_{\Delta T/2}$
George *et al*. [3] experiments	3.4	0.112	9.1	0.104
Chen & Rodi [1] recommendation	3.5	0.112	9.35	0.10
Shabbir & George [11] experiments	3.4	0.107	9.4	0.10
SKE	4.08	0.097	12.76	0.089
SKE_A	4.04	0.098	12.59	0.089
SKE_A*	4.04	0.098	12.55	0.089
SKE_B	3.32	0.132	8.48	0.119
SKE_B*	3.09	0.147	7.35	0.132
RKE	4.35	0.084	15.55	0.079
RKE_A	4.31	0.085	15.36	0.080
RKE_A*	4.3	0.085	15.31	0.080
RKE_B	3.74	0.103	11.78	0.098
RKE_B*	3.62	0.108	11.09	0.103
Hossain & Rodi [8] CFD A	-	0.079	-	0.076
Hossain & Rodi [8] CFD B	-	0.100	-	0.095
Hossain & Rodi [8] CFD C	3.50	0.109	8.22	0.100
Zhou *et al*. LES [28]	-	0.111	-	0.105

Van Maele & Merci also presented results for the streamwise and radial normal Reynolds stresses, $\overline{ww}$ and $\overline{uu}$ (not shown here). None of the models tested were capable of resolving the anisotropy in the normal stresses, although this is not unexpected since eddy-viscosity models like those tested by Van Maele & Merci were not designed to determine individual normal Reynolds stresses, only their sum, the turbulent kinetic energy. In the experiments, the streamwise stress was greater than the radial stress on the centreline, $\overline{ww} \approx 1.6\,\overline{uu}$. The linear $k - \varepsilon$ models on the other hand all gave $\overline{ww} \approx \overline{uu}$. Shear stresses were also not predicted very well and models overpredicted the peak value by up to 25%.

Plots of the *k*-profiles for standard and realizable models are shown in Figure 9. When normalized using similarity variables all of the models produced an off-axis peak in *k* which was not present in the experiments. Similar behaviour was observed in plane plumes by Yan & Holmstedt [53]. All standard $k - \varepsilon$ model variants underpredicted the centreline turbulent kinetic energy by around 15% whereas the realizable models were all in good agreement with the experiments. However, none of the model variants captured the correct shape of the *k*-profile.

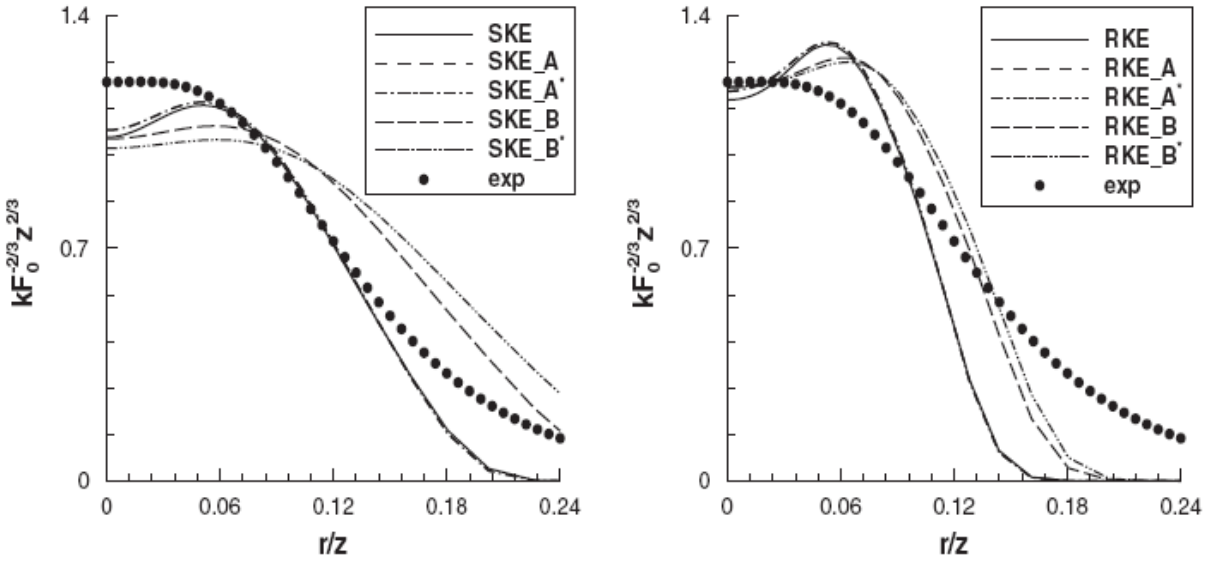

Figure 9 Profiles of turbulent kinetic energy, made dimensionless using similarity variables, from Van Maele & Merci [2].

3.2 Comparison to Other Model Predictions

To provide some comparison to other models' performance in this flow, the results of Yan & Holmstedt [53] are shown in Figure 10 for the George *et al*. [3] axisymmetric plume. The "standard model" they refer to is a standard $k - \varepsilon$ model with SGDH, whilst "this model" is a modified $k - \varepsilon$ model with GGDH that uses an algebraic relation for the Reynolds stresses where they appear in the production term, P_k. The standard model results are in good agreement with those obtained by Van Maele & Merci for the same case. The results obtained using their modified model appear to be better than those obtained by Van Maele & Merci for the standard $k - \varepsilon$ model with GGDH.

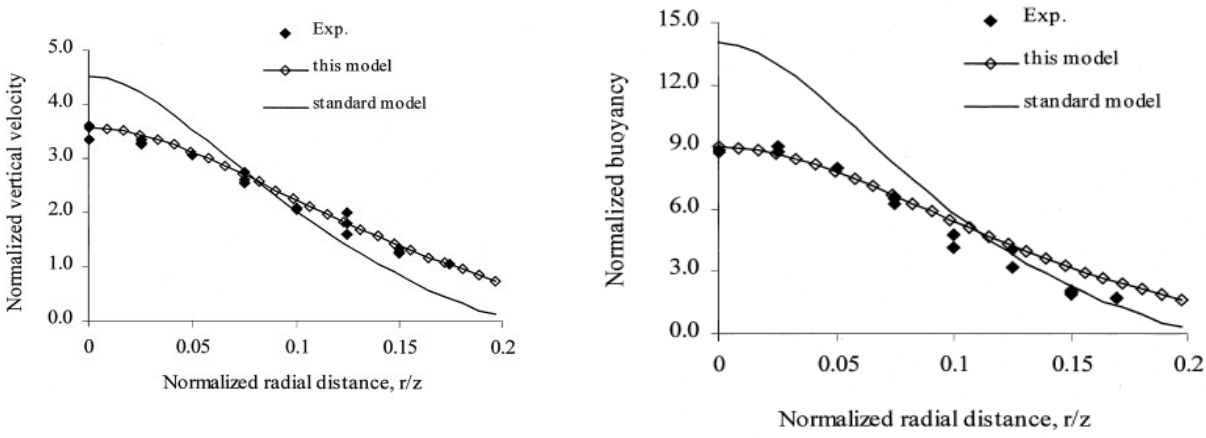

Figure 10 Normalized mean velocity and buoyancy profiles from Yan & Holmstedt [53]

The predictions of mean velocity and temperature from Hossain & Rodi [8] using an Algebraic Stress Model (ASM) are shown in Figure 11. As noted in Section 1.2.1, their model was derived from the differential stress model of Gibson & Launder [46]. Figure 11 shows that their predictions are in good agreement with the measurements of George *et al*. [3]. The predicted plume centreline values and half-widths using their model are shown in Table 5 (marked "Hossain & Rodi [8] CFD C"). These exhibit the best agreement with the measurements of George *et al*. [3] of all the model variants tested.

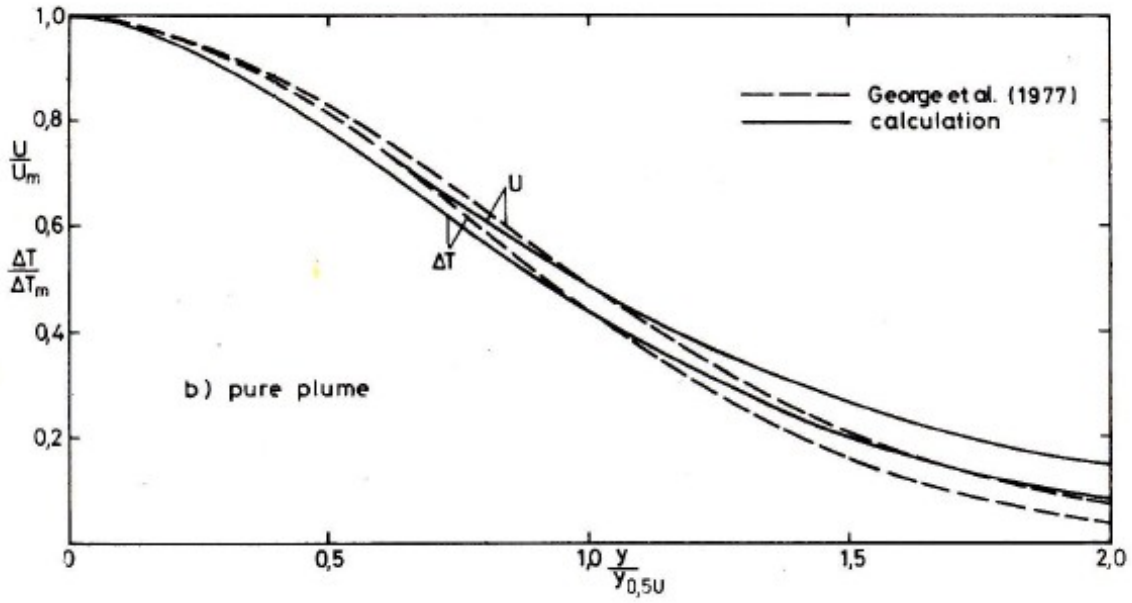

Figure 11 Normalized mean velocity and temperature profiles from Hossain & Rodi [8]

LES predictions from Zhou *et al*. [28] of the mean velocity and temperature for the experiments of George *et al*. [3] are shown in Figure 12. Very good agreement is obtained although this may be

partly a consequence of using centreline values to make the mean parameters dimensionless. Radial profiles of normalized RMS axial velocity and temperature were reported to produce a similar trend to that observed in the experiments, and turbulence levels within the experimental range [29], although the centreline dimensionless temperature fluctuation was approximately 0.45, in good agreement with the measurements of Papanicolaou & List [9] and Dai *et al*. [10], but slightly higher than the value of 0.40 reported by George *et al*. [28]. Plume spreading rates and centreline values were found to be strongly sensitive to the imposed turbulent fluctuations at the inlet plane in the LES model. Axial velocity fluctuations with an amplitude of 20% of the mean axial velocity were imposed at the inlet, with or without azimuthal forcing, to match the predicted location of the transition from laminar to turbulent flow to that observed in the experiments. In the experiments, however, the turbulence intensity at the inlet was reported to be approximately 0.5% [11].

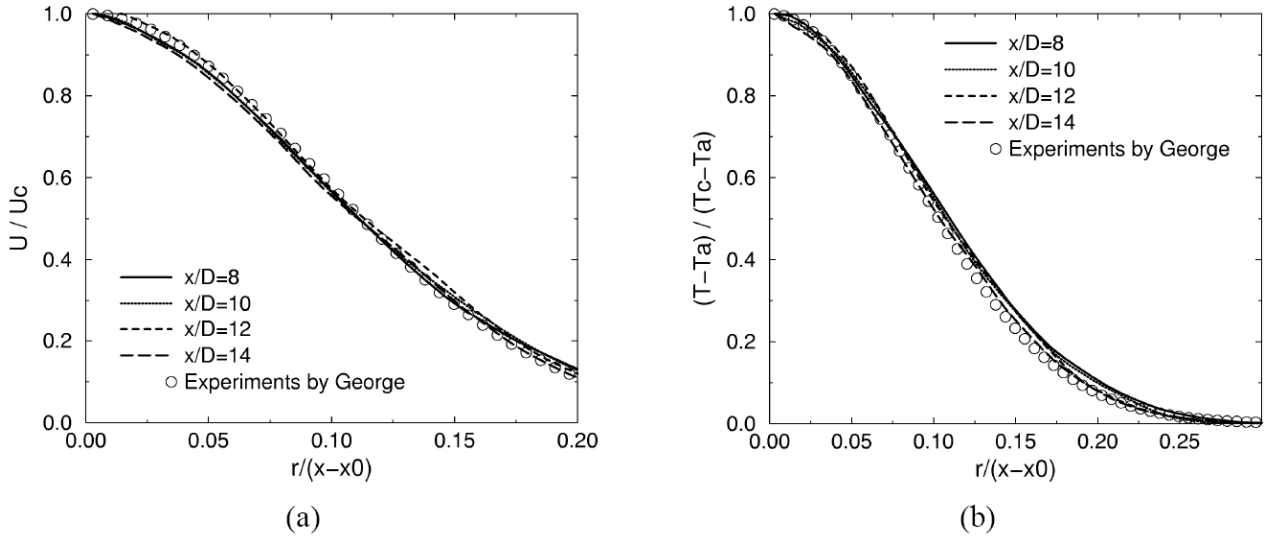

Figure 12 Radial profiles of (a) mean axial velocity, and (b) mean temperature at four axial positions compared to the experiments of George *et al*. [3], from the LES of Zhou *et al*. [28].

Figure 13 shows the dimensionless mean axial velocity profiles from Brescianini & Delichatsios [42]. Both the experimental results of George *et al*. [3] and Dai *et al*. [39] are shown. The basic model "ke1 Model A" is a standard $k - \varepsilon$ model with SGDH. Other model results shown include "keS Model B": a parabolic $k - \varepsilon$ model based on the work of Hanjalić & Launder [76] which retains both shear and normal-stress production terms, together with GGDH for the production term due to buoyancy; "keS Model C1": the same $k - \varepsilon$ model but with the streamwise turbulent scalar flux determined using the algebraic model of Hossain & Rodi [8]; and "keS Model C2": an extension of the C1 model that retains streamwise gradients of velocity and density. The three "keS" model variants all produce similar results that are in good agreement with the experiments of George *et al*. [3]. Interestingly, the standard $k - \varepsilon$ model with SGDH produces results in good agreement with the experimental data of Dai *et al*. [39] but in poor agreement with the data of George *et al*. [3]. Brescianini & Delichatsios [42] commented that the results of their assessment depend strongly upon which set of experiments are used for comparison.

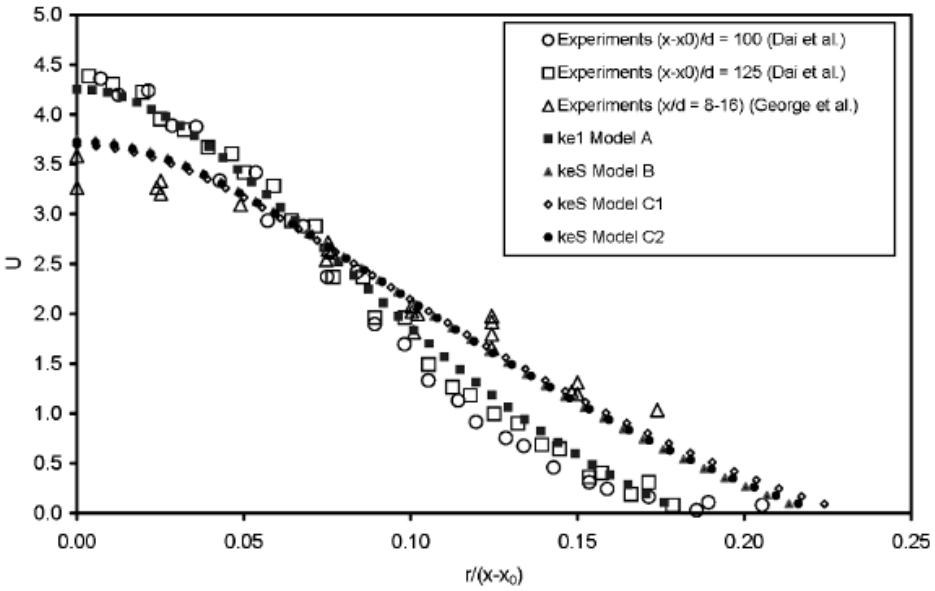

Figure 13 Mean axial velocity profiles from Brescianini & Delichatsios [42]. The quantity *U* on the y-axis is dimensionless and equivalent to $\left(W F_0^{-1/3} z^{1/3}\right)$ in Van Maele & Merci's notation.

3.3 Summary

Van Maele & Merci's [2] results for two different linear $k - \varepsilon$ models have been presented for the axisymmetric buoyant plume of George *et al*. [3]. Various modifications to the buoyancy treatment and other simplifications were tested. From this work, the following conclusions can be drawn:

- The Boussinesq approximation can be used to model the flow behaviour in far-field of buoyant plumes, where density differences are small. Nearer the source of buoyancy, where density differences are more appreciable, the approximation should be used with care. In Van Maele & Merci's [2] study it was shown to have no effect if SGDH is used, but had a noticeable effect with GGDH.

- The SGDH buoyancy-production term, G, is calculated using the streamwise temperature gradient which is small in this flow and the term therefore has little effect on the mean flow behaviour. As a consequence, when using SGDH the turbulent kinetic energy is underpredicted, the plumes have overly large centreline velocity and temperature values and do not spread sufficiently quickly.

- Using GGDH instead of SGDH improves the mean flow predictions.

- Neglecting the buoyancy source term, $S_{\varepsilon B}$, in the ε-equation has a relatively minor effect on the results with GGDH but can cause numerical stability problems. It is therefore not recommended to neglect this term.

- Van Maele & Merci assert that the realizable $k - \varepsilon$ model of Shih *et al*. [66] when combined with GGDH performs better than the standard $k - \varepsilon$ model with GGDH. However, the overall improvement shown in their results is relatively modest, if present at all.

- Better predictions of the mean flow behaviour in the far-field of buoyant plumes have been obtained using the more sophisticated $k - \varepsilon$ model of Yan & Holmstedt [53] and the ASM of Hossain & Rodi [8].

4 Best Practice Advice for the UFR

4.1 Key Physics

The key physics to be captured in this UFR is the self-similar behaviour of a spreading axisymmetric buoyant plume.

4.2 Numerical Modelling Issues

- The flow can be treated as axisymmetric.
- For a grid-independent resolution of the George *et al*. [3] plume, at least (40 × 100) grid nodes should be used in the (radial × axial) directions. At least 10 nodes should be used radially to resolve the plume source.
- Discretization schemes should be at least second-order accurate.
- For further advice on boundary conditions, see Section 3.4.3.

4.3 Physical Modelling

- Use of the standard $k - \varepsilon$ model with or without the common Standard Gradient Diffusion Hypothesis (SGDH) for the production term due to buoyancy, G, will probably result in overprediction of the centreline mean parameters, and underprediction of the spreading rate of the plume.
- To obtain more accurate plume predictions with a $k - \varepsilon$ model, use the Generalized Gradient Diffusion Hypothesis (GGDH) instead of the Standard Gradient Diffusion Hypothesis (SGDH). More refined models have been suggested which could further improve model predictions, see for example Hossain & Rodi [8].
- Do not neglect the buoyancy source term in the ε-equation as this can lead to problems with numerical stability.
- If you are considering only the far-field region of a buoyant plume, where density differences are small, the Boussinesq approximation can be used. If, however, your flow domain includes the region nearer the source of buoyancy where density differences are appreciable, avoid using the Boussinesq approximation.

- For cases where buoyancy is not as strong as in a plume, in the limit of a non-buoyant axisymmetric jet, be aware of the limitations of the standard $k - \varepsilon$ model. The spreading rate of a non-buoyant round jet is 15% lower than for a two-dimensional, plane jet. However, the standard $k - \varepsilon$ model predicts the spreading rate for round jets to be 15% *higher* than for the plane jets [67].

4.4 Application Uncertainties

In Van Maele & Merci's calculations, they substituted the streamwise normal stress in the GGDH expression for the production due to buoyancy, G, with the turbulent kinetic energy. They justified this ad-hoc modification on the basis that that the streamwise normal stress was underpredicted using a linear $k - \varepsilon$ model and therefore using k was more appropriate. However, this modification may not be appropriate in more complex flows where the flow direction is not aligned to one of the coordinate axes. The effect on Van Maele & Merci's results would have been to increase the buoyancy production term G. One could therefore expect to see a slightly less significant difference between SGDH and GGDH approaches without this ad-hoc modification.

Van Maele & Merci also did not report any tests that had been performed to assess the influence of the entrainment boundaries on the flow predictions. Ideally, simulations should have been performed using a smaller or larger domain to demonstrate that the presence of the entrainment boundaries had no affect on the solution.

4.5 Recommendations for Future Work

It is recommended that further experiments and a systematic re-evaluation of available data be undertaken to establish with confidence the self-similar behaviour of axisymmetric buoyant plumes, similar to the exercise undertaken 30 years ago by Chen & Rodi [1]. Both List [6] and Dai *et al*. [10] and have called into question whether the measurements by George *et al*. [3] were carried out sufficiently far from the source, in the region where self-similar behaviour exists. This issue was, however, dismissed by Shabbir & George [11][34].

Bibliography

1 Chen, C. J. and Rodi, W., *Vertical buoyant jets: a review of experimental data*, Pergamon, New York,1980

2 Van Maele, K. and Merci, B., Application of two buoyancy modified k-epsilon turbulence models to different types of buoyant plumes, *Fire Safety Journal*, 41, p.122-138, 2006

3 George, W. K. Jr., Alpert, R. L. and Tamanini, F., Turbulence measurements in an axisymmetric buoyant plume, *Int. J. Heat Mass Transfer*, 20, p.1145-1154, 1977

4 Gebhart, B., Jaluria, Y., Mahajan, R. L. and Sammakia, B., *Buoyancy-induced flows and transport*, Hemisphere Pub. Corp., New York,1988

5 Jaluria, Y., Hydrodynamics of laminar buoyant jets, in *Encyclopedia of Fluid Mechanics*, N. P. Cheremisinoff (Eds), Gulf Pub. Co., 1986

6 List, E. J., Turbulent jets and plumes, *Ann. Rev. Fluid Mech.*, 14, p.189-212, 1982

7 List, E. J., Mechanics of turbulent buoyant jets and plumes, in *Turbulent Buoyant Jets and Plumes*, Rodi, W. (Eds), Pergamon Press, 1982

8 Hossain, M. S. and Rodi, W., A turbulence model for buoyant flows and its application to vertical buoyant jets, in *Turbulent Buoyant Jets and Plumes*, W. Rodi (Eds), Pergamon Press, 1982

9 Papanicolaou, P. N. and List, E. J., Investigations of round vertical turbulent jets, *J. Fluid Mech*, 195, p.341-391, 1988

10 Dai, Z., Tseng, L.-K. and Faeth, G. M., Structure of round, fully-developed, buoyant turbulent plumes, *J. Heat Transfer*, 116, p.409-417, 94

11 Shabbir, A. and George, W. K., Experiments on a round turbulent buoyant plume, *J. Fluid Mech.*, 275, p.1-32, 1994

12 Yih, C.-S., Free convection due to a point source of heat, in *Proc. 1st U. S. Congr. Appl. Mech.*, E. Sternberg (Eds), ASME, 1951

13 Rouse, H., Yih, C. S. and Humphreys, H. W., Gravitational convection from a boundary source, *Tellus*, 4, p.201-210, 1952

14 Batchelor, G. K., Heat convection and buoyancy effects in fluids, *Quart. J. Roy. Met. Soc.*, 80, p.339-358, 1954

15 Morton, B. R., Taylor, G. I. and Turner, J. S., Turbulent gravitational convection from maintained and instantaneous sources, *Proc. Roy. Soc. Lond.*, A234, p.1-23, 1956

16 Delichatsios, M. A., On the similarity of velocity and temperature profiles in strong (variable density) turbulent buoyant plumes, *Combust. Sci and Tech.*, 60, p.253-266, 1988

17 Rooney, G. G. and Linden, P. F., Similarity considerations for non-Boussinesq plumes in an unstratified environment, *J. Fluid Mech.*, 318, p.237-250, 1996

18 Scase, M. M., Caulfield, C. P., Dalziel, S. B. and Hunt, J. C. R., Time-dependent plumes and jets with decreasing source strength, *J. Fluid Mech.*, 563, p.443-461, 2006

19 Scase, M. M., Caulfield, C. P. and Dalziel, S. B., Boussinesq plumes and jets with decreasing source strengths in statified environments, *J. Fluid Mech.*, 563, p.463-472, 2006

20 Delichatsios, M. A., Time similarity analysis of unsteady buoyant plumes in neutral surroundings, *J. Fluid Mech.*, 93, p.241-250, 1979

21 Heskestad, G., Virtual origins of fire plumes, *Fire Safety Journal*, 5, p.109-114, 1983

22 Heskestad, G., Engineering relations for fire plumes, *Fire Safety Journal*, 7, p.25-32, 1984

23 Zukoski, E. E., Kubota, T. and Cetegen, B., Entrainment in Fire Plumes, *Fire Safety Journal*, 3, p.107-121, 1981

24 Fang, J. and Yuan, H.-Y., Experimental measurements, integral modeling and smoke detection of early fire in thermally stratified environments, *Fire Safety Journal*, 42, p.11-24, 2007

25 Schmidt, W., Turbulente ausbreitung eines stromes erhitzter luft, *Z. Angew. Math. Mech.*, 21, p.265-278 and p.351-363, 1941

26 Linden, P. F., Convection in the environment, in *Perspectives in Fluid Dynamics*, G. K. Batchelor, H. K. Moffat & M. G. Worster (Eds), Cambridge University Press, 2000
27 Diez, F. J. and Dahm, W. J. A., Effects of heat release on turbulent shear flows. Part 3 Buoyancy effects due to heat release in jets and plumes, *J. Fluid Mech.*, 575, p.221-255, 2007
28 Zhou, X., Luo, K. H. and Williams, J. J. R., Large-eddy simulation of a turbulent forced plume, *Eur. J. Mech. B - Fluids*, 20, p.233-254, 2001
29 Zhou, X., Luo, K. H. and Williams, J. J. R., Study of density effects in turbulent buoyancy jets using large-eddy simulation, *Theoret. Comput. Fluid Dynamics*, 15, p.95-120, 2001
30 Cetegen, B. M., Behavior of naturally unstable and periodically forced axisymmetric buoyant plumes of helium and helium-air mixtures, *Phys. Fluids*, 9, p.3742-3752, 1997
31 Shabbir, A. and George, W. K., Energy balance measurements in an axisymmetric buoyant plume, in *Proc. 6th Symp. on Turbulent Shear Flows*, (Eds), , 1987
32 Shabbir, A., *An experimental study of an axisymmetric turbulent buoyant plume and investigation of closure hypotheses*, , Dept. of Mech. & Aero. Eng., University at Buffalo 1987
33 Shabbir, A. and Taulbee, T. B., Evaluation of turbulence models for predicting buoyant flows, *J. Heat Transfer*, 112, p.945-951, 1990
34 Shabbir, A. and George, W. K., Experiments on a round turbulent buoyant plume, in *NASA Technical Memorandum 105955*, (Eds), , 1992
35 Papantoniou, P. N. and List, E. J., Large scale structure in the far field of buoyant jets, *J. Fluid Mech.*, 209, p.151-190, 1989
36 Papanicolaou, P. N. and List, E. J., Statistical and spectral properties of tracer concentration in round buoyant jets, *Int. J. Heat Mass Transfer*, 30, p.2059-2071, 1987
37 Dai, Z., Tseng, L.-K. and Faeth, G. M., Velocity statistics of round, fully developed buoyant turbulent plumes, *J. Heat Transfer*, 117, p.138-145, 1995
38 Dai, Z., Tsend, L.-K. and Faeth, G. M., Velocity/mixture-fraction statistics of round, self-preserving buoyant turbulent plumes, *J. Heat Transfer*, 117, p.918-926, 1995
39 Dai, Z., Krishnan, S. K., Sangras, R., Wu, J. S. and Faeth, G. M., Mixing and Radiation Properties of Buoyant Luminous Flame Environments, in *NIST-GCR-96-691*, (Eds), National Institute for Standards & Technology, 1996
40 George, W. K., Governing equations, experiments and the experimentalist, *Experimental Thermal and Fluid Science*, 3, p.557-566, 1990
41 Dai, Z. and Faeth, G. M., Measurement of the structure of self-preserving round buoyant turbulent plumes, *J. Heat Transfer*, 118, p.493-495, 1996
42 Brescianini, C. P. and Delichatsios, M. A., New evaluation of the k-epsilon turbulence model for free buoyant plumes, *Numerical Heat Transfer, Part A*, 43, p.731-751, 2003
43 Heskestad, G., Dynamics of the fire plume, *Phi. Trans. Roy. Soc.*, 356, p.2815-2833, 1998
44 Shabbir, A. and Taulbee, D. B., Experimental balances for the second moments for a buoyant plume and their implication on turbulence modeling, *Int. J. Heat Mass Transfer*, 43, p.1777-1790, 2000
45 Yao, X. and Marshall, A. W., Qantitative salt-water modeling of fire-induced flow, *Fire Safety Journal*, 41, p.497-508, 2006
46 Gibson, M. M. and Launder, B. E., Ground effects on pressure fluctuations in the atmospheric boundary layer, *J. Fluid Mech.*, , p.491-511, 1978
47 Rodi, W., *The prediction of free turbulent boundary layers by use of a two-equation model of turbulence*, , PhD Thesis, University of London, UK 1972
48 Nam, S. and Bill, R. G. Jr., Numerical simulation of thermal plumes, *Fire Safety Journal*, 21, p.213-256, 1993
49 Launder, B. E. and Spalding, D. B., *Mathematical models of turbulence*, Academic Press, London,1972
50 Hara, T. and Kato, S., Numerical simulation of thermal plumes in free space using the standard

k-epsilon model, *Fire Safety Journal*, 39, p.105-129, 2004
51 Yokoi, S., Study on the prevention of fire-spread caused by hot upward current, in *Building Research Institute Report No. 34*, (Eds), , 1960
52 Daly, B. J. and Harlow, F. H., Transport equations in turbulence, *Phys. Fluids*, 13, p.2634-2649, 1970
53 Yan, Z. and Holmstedt, G., A two-equation model and its application to a buoyant diffusion flame, *Int. J. Heat Mass Transfer*, 42, p.1305-1315, 1999
54 Davidson, L., Second-order correction of the k-epsilon model to account for non-isotropic effects due to buoyancy, *Int. J. Heat Mass Transfer*, 33, p.2599-2608, 1990
55 Malin, M. R. and Younis, B. A., Calculation of turbulent buoyant plumes with a Reynolds stress and heat flux transport closure, *Int. J. Heat Mass Transfer*, 33, p.2247-2264, 1990
56 Gibson, M. M. and Younis, B. A., Modelling the curved turbulent wall jet, *AIAA J.*, 20, p.1707-1712, 1982
57 Gibson, M. M. and Younis, B. A., Calculation of swirling jets with a Reynolds stress closure, *Phys. Fluids*, 29, p.38-48, 1986
58 Gibson, M. M. and Younis, B. A., Calculation of boundary layers with sudden transverse strain, *ASME J. Fluids Eng.*, 108, p.470-475, 1986
59 Craft, T. J., Ince, N. Z. and Launder, B. E., Recent developments in second-moment closure for buoyancy-affected flows, *Dynamics of Atmospheres and Oceans*, 23, p.99-114, 1996
60 Cresswell, R., Haroutunian, V., Ince, N. Z., Launder, B. E. and Szczepura, R. T., Measurement and modelling of buoyancy-modified elliptic turbulent flows, in *Proc. 7th Symp. on Turbulent Shear Flows*, (Eds), , 1989
61 el Baz, A., Craft, T. J., Ince, N. Z. and Launder, B. E., On the adequacy of the thin-shear-flow equations for computing turbulent jets in stagnant surroundings, *Int. J. Heat Fluid Flow*, 14, p.164-169, 1993
62 Magi, V., Iyer, V. and Abraham, J., The k-epsilon model and computed spreading rates in round and plane jets, *Num. Heat Transfer, Part A*, 40, p.317-334, 2001
63 Haroutunian, M. and Launder, B. E., Second-moment modelling of free buoyant shear flows: a comparison of parabolic and elliptic solutions, in *Proc. IMA Conf. on Stably Stratified Flow and Dense Gas Dispersion*, (Eds), , 1986
64 Rouse, J., Yih, C. S. and Humphrey, R. W., Gravitational convection from a boundary source, *Tellus*, 4, p.201-210, 1952
65 Jones, W. P. and Launder, B. E., The prediction of laminarization with a two-equation model of turbulence, *Int. J. Heat Mass Transfer*, 15, p.301-314, 1972
66 Shih, T. H., Liou, W. W., Shabbir, A., Yang, Z. and Zhu, J., A new k-epsilon eddy-viscosity model for high Reynolds number turbulent flows, *Comput. Fluids*, 24, p.227-238, 1995
67 Pope, S. B., An explanation of the round-jet/plane-jet anomaly, *AIAA Journal*, 16, p.279-281, 1978
68 Kato, M. and Launder, B. E., The modelling of turbulent flow around stationary and vibrating cylinders, in *Proc. 9th Symposium on Turbulent Shear Flows*, (Eds), , 1993
69 Wilcox, D. C., *Turbulence Modelling for CFD*, DCW Industries, ,1993
70 Ince, N. Z. and Launder, B. E., On the computation of buoyancy-driven turbulent flows in rectangular enclosures, *Int. J. Heat Fluid Flow*, 10, p.110-117, 1989
71 Rodi, W., *Turbulence models and their application in hydraulics*, A.A. Balkema, Rotterdam, , 1980
72 Markatos, N. C., Malin, M. R. and Cox, G., Mathematical modeling of buoyancy-induced smoke flow in enclosures, *Int. J. Heat Mass Transfer*, 25, p.63-75, 1982
73 Worthy, J., Sanderson, V. and Rubini, P., Comparison of modeified k-epsilon turbulence mdels for buoyant plumes, *Numerical Heat Transfer B: Fundamentals*, 39, p.151-165, 2001
74 Chassaig, P., Antonia, R. A., Anselmet, F., Joly, L. and Sarkar, S., *Variable density fluid*

turbulence, Kluwer Academic Publishers, Dordrecht, MA,2002
75 O'Hern, T. J., Weckman, E. J., Gerhart, A. L., Tieszen, S. R. and Schefer, R. W., Experimental study of a turbulent buoyant helium plume, *J. Fluid Mech.*, 544, p.143-171, 2005
76 Hanjalić, K. and Launder, B. E., Sensitizing the dissipation equation to irrotational strains, *J. Fluids Eng.*, 102, p.34-40, 1980